Article:
Peterson, EL and Shafagh, I (2022) Evaluation of diaphragm wall heat exchanger potential. Energy and Buildings, 266. 112107. ISSN 0378-7788

https://doi.org/10.1016/j.enbuild.2022.112107

Evaluation of diaphragm wall heat exchanger potential

Eric Laurentius Peterson [12]* and Ida Shafagh [1]
[1] School of Civil Engineering, University of Leeds, Leeds, West Yorkshire LS2 9JT United Kingdom
[2] School of Biology, University of Leeds, Leeds, West Yorkshire LS2 9JT United Kingdom
* Corresponding author: e.peterson@leeds.ac.uk

Abstract:

Diaphragm wall foundations adapted for use as ground heat exchangers are an attractive proposition to achieve low-carbon heating and cooling with heat pumps in larger non-domestic buildings. As the extent of a diaphragm wall installation is driven by geotechnical questions and the number of storeys, key system design considerations are the peak and seasonal capacity of the ground heat exchanger and the proportion of the building demands that can be satisfied. Dynamic simulations of prototypical office buildings in a range of climatic conditions have been used to analyse heat exchange potentials using a Dynamic Thermal Network (DTN) heat exchanger model. Systematic evaluations of the time-dependent heat fluxes between three boundaries (heat exchanger, basement, ground surface) have been made to maximize heat exchange potentials and overall system efficiency given temperature constraints over 20 years operation. This has allowed maximum heat exchange potentials to be evaluated for a range of design parameters and climates to enable preliminary design of diaphragm wall heat exchanger systems and assessment of hybridized solutions. Considering short timescale dynamic effects suggests peak heat exchange rates higher than previously reported. In some climates seasonal operation is found to be constrained by temperature limits according to ground thermal properties.

Keywords: screen wall heat exchanger; diaphragm wall heat exchanger; foundation heat exchanger

1. Introduction

This paper reviews literature and contributes original research findings evaluating the capacity of diaphragm wall foundations adapted for use as ground source heat exchangers. The context is that various types of ground source heat exchangers can serve heating and cooling loads of buildings with better inter-seasonal performance than air-source heat pumps and air-

conditioners. This paper's objective is to evaluate the potential of vertical diaphragm wall heat exchanger (DWHE) integration into ground-source heating and cooling systems without freezing or overheating the basement of the associated building. Original results are compared with others'.

The original research contributed by this paper is a series of simulations of a heatpump and chiller responding to building heating and cooling loads in various climates with various ground soil conductivities compared by varying the number of activated DWHE modules. The DWHE model was validated in Barcelona, Spain, and implemented as a simulation component type in TRNSYS17 [1].

The results are described, discussed and justified in terms of the local climate, soil conductivity, and the intermittency of heating and cooling loads imposed by the HVAC system.

Background literature describes how ground source heat exchangers, heat pump systems, and space heating-cooling systems interact. A unique focus of the present literature review is to compare DWHE performance in terms of a common denominator – the meters of wall (m_h) measured horizontally. This is distinct from the convention of normalising performance of U-tube bore heat exchangers and thermal piles by vertical dimension meters (m_v). DWHE performance is further normalized by the thermally active depth of walls such that performance is proportional to vertical area exposed to soil on at least one side, measured in square meters (m^2).

The present review is tabulated as a comparison of DWHE capacity as heat source and/or sink per square meter and dividing these by the active length of each. Table 1 also discloses overall active depth of each DWHE as well as the portion embedded below the lowest basement floor.

A geothermally activated building structure - also known of as foundation heat exchanger (FHX) is useful in dense urban settings. Geoexchange systems historically depended on borehole heat exchangers or horizontal pipe networks buried under adjoining parking lots and gardens. This has limited application in dense urban settings until development of pipework integration with steel-reinforced concrete piles required to support high-rise buildings: so-called energy piles. Diaphragm

walls provide an additional opportunity to integrate ground-source heat exchangers into the perimeter basement retaining walls of high-rise buildings. A diaphragm wall heat exchanger (DWHE) is also known as a screen wall heat exchanger. DWHEs and energy piles are examples of FHXs.

The use of building foundations as heat exchangers has developed cautiously with concern for cyclic thermal impact on structural safety performance [2-4]. Some literature has been thermo-mechanically focused on the dilemma of increasing energy density and thermal expansion of the structural steel-reinforced concrete matrix that integrate with the heat exchange fluid pipework. A few studies (such as the present paper) have been focused on capacity to provide heat sources and sinks as dynamically demanded in the operation of building services. Thermo-hydro-mechanical analysis could correct initial assumptions in the process of designing retraining walls [5, 6], especially if thermal activation can be enhanced beyond what has been demonstrated to date [7].

Geoexchange , or ground coupled heat pump (GCHP), systems are generally more efficient than conventional air-source heat-pump / air-conditioners[8, 9], but heretofore the capital expense and land-required for ground-source heat exchangers have often been problematic[10]. Effective GCHP system controls are complex[11], with further discussion in sub-section 2.1 of methods.

While energy piles are the more conventional foundation heat exchanger (FHX) elements for geoexchange systems, diaphragm wall heat exchangers have seen less exploitation in buildings and infrastructure [10] until a few case studies emerged in Austria, China, and the UK [12]. Early case studies involved the retaining walls of underground railway tunnels. With respect to hot climate developments, DWHEs have been installed at the Shanghai Museum of Natural History [3] – but without published post-occupancy studies it is not known if this installation proved to be a sustainable heat sink. Meanwhile the last 12 years of research and development have started to address problems of integrating SWHEs into building perimeter foundations [1, 13-15]. Ongoing there have been more studies focused on heat sink (rejection of heat injected into the earth) via U-tube bore fields [16, 17], or cast into structural foundation piles and caissons [2, 18].

While borehole heat exchangers are known to perform heat extraction/rejection circa 30-100 W/m_v, foundation thermal piles have performed in the lower of range 40-50 W/m_v [13]. Both of these typologies behave cylindrically as a vertical "line-source" [12], so performance is proportional by embedded depth measured vertically in meters (m_v).

With respect to U-tube cast into foundation piles, performance is assumed to be scalable pro-rata with respect to vertical meters (m_v) of embedment. VDI general guidance for heat extraction from poor to normal soil conditions (1.5 to 3.0 W/m·K thermal conductivity) in Central Europe [19, 20] suggests U-tube heat source capacity for space heating vary 25-60 W/m_v , but drops to 20-50 W/m_v if service hot water demand is included. Those guidelines do not account for the higher potential capacity of alternating heating and cooling (extraction intermixed with rejection) associated with reverse-cycle HVAC systems. Subsequent research suggested heat extraction capacity guidelines should be adjusted depending on pile diameter and L/D ratio [21].

1.1. Horizontal ground heat exchanger (HGHE) – an ideally two-dimensional typology

While the opportunity to integrate a DWHE into a vertical basement wall is the focus of the present review, there is a greater body of literature describing another planar heat exchanger typology. This is the horizontal ground heat exchangers (HGHE), comprising pipework loops buried below frost level. VDI guidelines for central Europe suggest that HGHEs can provide 16 to 24 W/m² of heat extraction for 2400 hours per annum from moist cohesive soil, but only 8 W/m² in dry non-cohesive soil [22]. Scholarly literature describes how outdoor ground heat exchangers, heat pump systems, and space heating-cooling systems interact, involving various types of ground-source heat exchangers. HGHEs may have been more generally applied because they do not involve specialist drilling, only depending on a land area covered with suitable soil [23].

Esen, et al.'s research program Firat University, Elaziğ, Turkey has demonstrated HGHE performance in a Mediterranean-influenced hot-summer humid continental climate, back-filled one or two meters. Their energy and exergy analysis shows that HGHE performance for heat pumping increases when the ground temperature is higher [8]. Techno-economic appraisal of heating [24] and comparison space cooling [9] show that HGHE/heat-pump systems demonstrated at are superior to air-source systems. In evaluation of HGHE performance, numerical finite difference and experimental analysis agreed [25].

Vector and neural network methods [11, 26] as well as modelling with adaptive neuro-fuzzy interface systems found HGHE horizontal layout of serpentine arrangement per meter (m_p) of 16 mm Ø pipework with 0.3 m_h spacing resulted in 7 to 8 W/m_p (24 to 27 W/m^2) capacity, depending on installed depth of installation [27] – VDI [22] implies that the local soil was suitably conductive. Artificial neural networks and adaptive neuro-fuzzy interface systems [28], statistical weighting [29], and fuzzy logic [30] were trained to predict performance of their HGHE/Heat-pump system. Horizontal slinky [31] and vertical slinky [32] performance of ground source heat exchangers integrate well with solar heat source for climate control of greenhouses in Eastern Turkey's Dsa Köppen climate at Firat University.

While vertical borehole heat exchangers are currently most popular, HGHEs are simple to design and install if suitable land is available[23]. The two-dimensional planar performance of a HGHE is naturally normalised by the area, with reference to the depth of soil backfilled on the upper side. Beware that the heat transfer dynamics becomes three-dimensional by tilting a planar heat exchanger vertically and only backfilling on the extrados side when integrated into a soil retaining wall, tunnel, or basement. So, this review now turns to performance of a vertical DWHE, integrated into foundations at the perimeter of a building.

1.2. Review of guidelines arising from studies of vertical DWHE capacity

While the forgoing review of HGHE demonstrations at Firat University proves the systemic advantages for ground source heating and cooling, it does not provide quantitative guidance on the capacity of vertically installed DWHEs. Therefor the present paper includes a new comparative review of experimental and simulated performance of DWHEs. The present aim is to provide guidelines of the rates of DHWE capacity for heating and cooling. The results could be used to consider the opportunity at relatively small additional capital expense of activated DWHEs when foundation walls are installed [2, 33]. This is to complement better understood opportunities to exploit structural caissons and piles as ground source heat exchangers by including vertical U-tube pipework [34].

Reviews show that energy piles can exchange between 40 and 120 W/m_v normalized as line-sources, while diaphragm energy walls of tunnels exchange 10 to 50 W/m² normalized by area [35]. With regard to passive cooling air via diaphragm walls, peak cooling capacity at ambient 32°C was reported as 45 W/m² of ground coupling area [36]. Focused on a cooling dominated climate study of water chiller capacity, thermal pile heat rejection capacity was projected to decrease after 5 years 38–43 W/m_v and 35–37 W/m_v for two cases [18]. The present review and original research aims to provide guidance to estimate how much mechanical chiller heat rejection in summer – as well as heat pump extraction in winter – are sustainably satisfied for a given installation of diaphragm walls, to complement the capacity of other FHXs that may be conveniently exploited, such as piles.

Application of energy tunnels in urban environments are capable of 73 W/m² heat rejection [37]. A diaphragm energy wall system considered in another study allowed exchange between 20 and 25 W/m² when ground water is static, that rises up to 40-50 W/m² with suitable underground water flow [38]. Numerical simulation of diaphragm wall heat transfer rates was confirmed circa 20 W/m² [12]. In retaining wall simulations, 15-20 W/m² heat rejection was reported [39].

In order to develop a sustainable geoexchange system it is necessary – having established building heating and cooling demand profile – to estimate how much heat exchanger capacity is needed to seasonally store heat and coolth. One key performance indicator is heat flux per unit area ($m_h \times m_v$) of diaphragm wall – capacity per horizontal width, divided by vertical length of pipe (VL_{pipe}).

Integrating heat exchanger sections (Figure 1) into reinforcement steelwork enables a concrete diaphragm wall to also function as a DWHE. Diaphragm walls are soil retaining walls for deep basements and underground tunnels, with the steel-reinforcement "rebar cage" panels assembled horizontally before tilting with a crane. Installation involves cutting a deep/narrow trench in the ground and lowering the assembly into the excavated slot, which may be temporarily flooded with bentonite slurry, before displacement with concrete. DWHE adaptation of rebar cages was used in construction of a large tertiary building in Barcelona, Spain[1] – demonstrated by GEOTeCH Project YouTube video [40]. Table 1 notes that vertical pipe depth, including extension below basement level, has varied among research studies, which compares prorate horizontal meters (m_h) extent of foundation cross sections such as Figure 2.

Figure 2 shows DWHE heat exchanger pipework is cast within a thin layer, relatively close to the outside of screen wall panels so there is enhanced thermal conduction with the extrados soil. Regarding DWHE typologies, cast concrete diaphragm walls contain a network of serpentine pipework that don't behave as a line-source. DWHE performance is typically normalized by unit of planar area normal to heat flux but would be better compared per unit horizontal length of foundation perimeter for particular geometries of embedment below the basement (Table 1).

Publications exploring potential of increasing heat exchange by increasing pipe diameter have not been found, while most studies have nominated 25 mm outside diameter pipe [3, 12, 14, 35, 37, 41-45]. The present authors suppose larger tubing would require greater investment in concrete to ensure covering and such would increase pipe-spacing, dictated by the practicalities of creating 180° bends return bends [41] could diminish performance. Fitting multiple vertical W loops

of heat exchange tubing are more effective than multiple horizontal switchbacks with a return riser on the end [41].

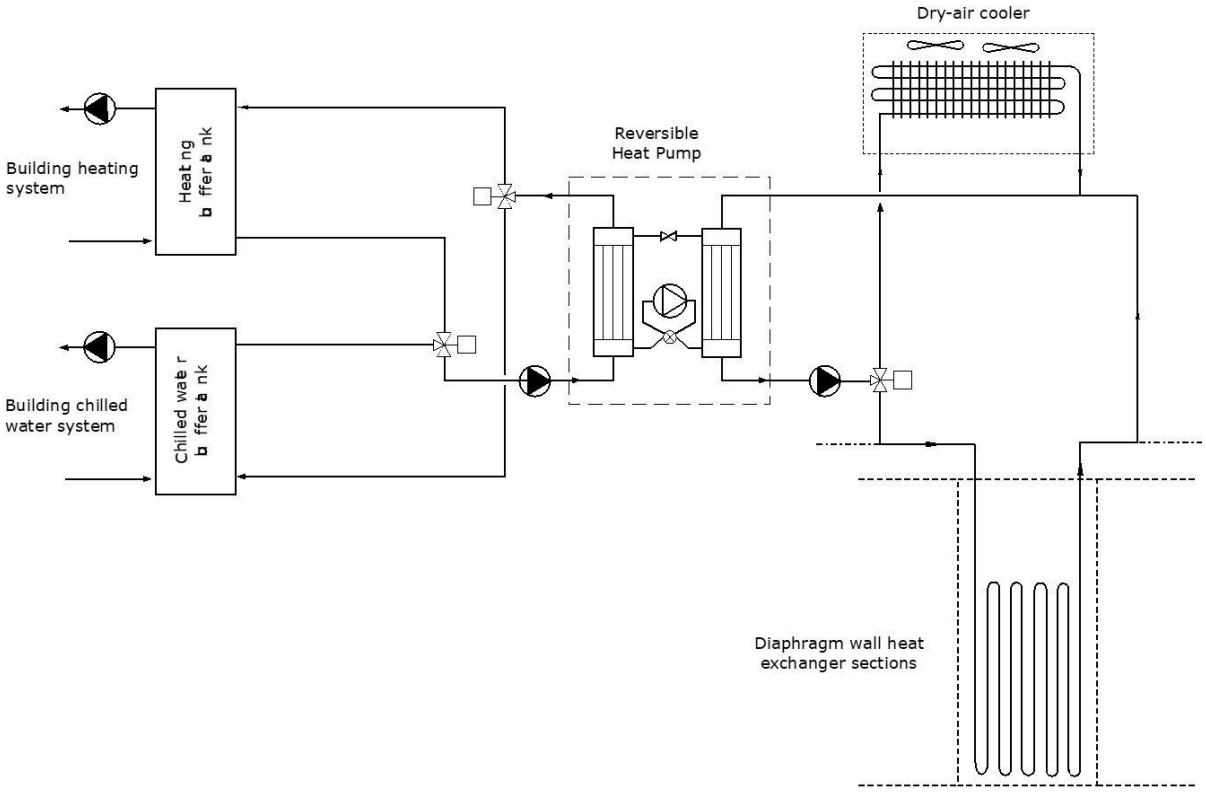

Figure 1. Four-pipe heatpump/chiller with demand-side buffer tanks and hybrid source-side heat exchangers. The air-cooled mode is not considered in the current paper. Serpentine diaphragm wall heat exchanger sections are repeated in parallel with common entering and leaving headers. Graphic courtesy Simon Rees, Professor of Building Energy Systems, University of Leeds.

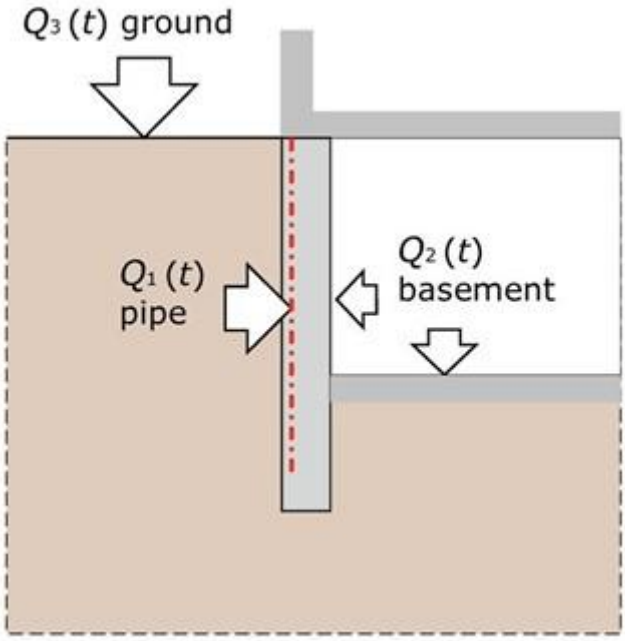

Figure 2. Definition of the three boundary surfaces and corresponding time-varying heat fluxes in a Dynamic Thermal Network (DTN) representation of a diaphragm wall ground heat exchanger. Reproduced from Shafagh et al. [1] Creative Commons (CC BY 4.0).

Vertical U- and W-tubes cast into a diaphragm retaining wall modules of the Shanghai Museum of Natural History were initially rejecting over 120 W/m_v but soon dropped below 80 W/m_v and decayed to 50 W/m_v after 2-days continuous operation [3]. This is equivalent to 67 W/m^2 if their stated 750 mm horizonal spacing between the vertical pipe sections of the U-tube were the diaphragm wall module width. Their test conditions – 0.6 m/s through 20.4 mm internal (nominal φ25 mm with 2.3 mm wall) polythene 100 pipe – are somewhat comparable to the current paper's default geometry (last entry in Table 1). It is unclear if their lateral boundary conditions were periodic – such that performance would be consistent with an infinite series of vertical elements spaced around the perimeter of a building. The floor plan in their paper[3] scales to indicate a total perimeter length of about 670 m_h including subway and basement walls, which confers with their stated n=452 foundation heat exchanger modules if each is 1500 mm wide (1.5 m_h/n).

There has been a mixture of monitoring and modelling studies of DWHE performance (Table 1). In-situ thermal response testing have been limited a few hours, with a couple of exceptions [38, 46], and so simulations are necessary to resolve inter-seasonal and inter-annual balances [41].

The vertical area of foundations may be a reasonable common denominator for comparing DWHE performances – except for complexities of aspect-ratio embedment depth of footings versus the height of basement walls, and that backfilling is not necessarily to the same elevation on either side. Consequently, a response factor approach is useful to capture cross sectional geometries (Figure 2) of the transient heat transfer problem [1, 47, 48]. This reduces subsequent computation time by orders of magnitude less than bespoke finite element modelling each foundation design.

Results are presented in the results section of this paper for a range of higher and lower soil conductivities at other European locations as well as Barcelona and Amsterdam. These two locations are included in Table 1 as median representatives of Mediterranean (Cfb) and oceanic (Csa) climates. Table 1 normalizes the results of five previously published studies of DWHE capacity by the horizontal length of each particular cross section. Area of thermally activated diaphragm wall might not be a better basis for comparison since each case study had a unique aspect ratio of basement wall to overall activated depth, ranging from 75% to 50%. Additionally, Table 1 illustrates that the present paper has modelled a design with 45% basement aspect ratio – whereby 55% of the overall activated diaphragm wall is backfilled on both sides of the building's perimeter foundation.

The contributions and limitations of the present work are incremental in the context of others [12, 15, 38, 41, 46], as each study has assumed a unique DWHE geometry. Uniquely the present work has integrated our DEFAULT DWHE with hourly simulations of building services of a prototypical multistorey office building floor plan so that one can estimate how many replicated stories could be sustainably served by geoexchange year after year without ever freezing in winter. Furthermore the study imposes an upper limit in summer to prevent basement screen walls from exceeding 37.8°C, while others[38, 41] assumed adiabatic conditions at ventilated surfaces.

Table 1: Diaphragm retaining wall heat exchanger capacity literature review normalised by meters of width of each module (m_h)

reference	Peak performance	W_{peak}/m_h	MJ_a/m_h	Extended performances	W/m^2	W/m_h	MJ_a/m_h	vertical piping	basement Embedment	aspect ratio
[3, 14] Xia, Sun Shanghai	Initial rate -80 W/m^2 -120 W/m_v	-2990	-94,000 extrapolated	After 48 hr -72.7 W/m_v	-48	-1811	-57,000 extrapolated	37.5 m_v	18.5 m_v	51%
[41] Makasis & Narsilio † Melbourne	Balance-7.5/+3.3 W/m^2 -vs- Realistic unbalanced |heating| < |cooling|	-150/+67 -11 +83		Balanced -vs- Realistic T_{max} > 45°C	±1.9 -3.3 +7.5	±39 -67 +150	±1,222 -2100 +4700	20 m_v	5 m_v	75%
[38] Barla ‡ † Torino, Italy	Summer -25.2 W_{peak}/m^2	-391	-12,000 extrapolated	Summer	-9.6	-149	-4,700 extrapolated	15.5 m_v	6 m_v	61%
	Winter +20.4 W_{peak}/m^2			Winter	+6.9	+107	+3,400 extrapolated			
[15] Sterpi Tradate, Italy	Monitoring winter performance			Average performance	+13.9	+70	+2,200 extrapolated	15.2 m_v	5 m_v	67%
[12] di Donna et al. analysis	winter +110 W_{peak}/m^2 summer -154 W_{peak}/m^2	+2,200 -3,100	+69,000 -97,000 extrapolated	For dry soils, groundwater	6 to 32, gw 48	60 to 320, 480	1,300 to 6,700, gw 15,000	10 m_v	5 m_v	50%
[46] Zannin, et al. Geneva	7 kW/(21.6 m_v×2.5 m_h) = 130 W_{peak}/m^2	2,800	88,000 extrapolated	Winter Spring	+25 -85	+540 -1800	+17,000 -58,000	21.6 m_v	7.9 m_v	63%
[*] Barcelona	Max summer ½hour -52 to -84 W_{peak}/m^2	**-755 to -1,256**	-24,000 -34,000	Safe annual injection	-4 to -5	-64 to -75	**-2,030 to -2,372**	14.6 m_v	8.1 m_v	45%
[*] Amsterdam	Max winter ½hour +17 to +32 W_{peak}/m^2	**+248 to +467**	+8,000 +15,000	Safe annual Extraction	+0.4 to +0.7	+6 to +11	**+196 to +343**			

‡ results tabulated above ignore groundwater, but such significantly improves performance [38, 49].

† [38, 41] assumed basement walls were insulated on the intrados side, without heat transfer to air.

* Range of simulation results of the present paper include heat transfer through basement walls with 0.9 – 2.2 W/(m·K) range of soil conductivities.

1.3. Integration of source-side network into the design of building services

There is a dynamic balance between the heating-cooling demands of the building, the capacity of chiller/heat pump plant, and the “source side” system of extracting heat from the ground in winter and rejecting waste heat to the ground and ambient air during summer.

In the analysis of the thermal demand of the building, there can be a partial satisfaction of demand with district heating or cooling schemes, or provision of auxiliary on-site plant. There may be demand-side measures such as Passive-Haus construction standards – but such are not effective to manage overheating in summer in warm climates. Therefore, it could be necessary to partially supplement cooling capacity with dry air-coolers or wet cooling towers.

Balancing is necessary to prevent freezing or thermal pollution of the ground –determined with simulation of annual heat extraction over many winters, each sequentially countered by annual heat rejection for as many summers. Multi-decadal life-cycle of any proposed heat pump installation should meet building loads without ever freezing pipework. Also for the present study an upper guideline for the highest condensing water temperature was adopted to align with human fever temperature 37.8°C. It could be dangerous if foundation heat exchangers in basement foundation walls operated frequently above this guideline. There may be consideration of the possibility of operating above this threshold in un-inhabited foundation walls. Thus a 1°C minimum temperature of water leaving heat pump evaporator is the primary criteria, while there may be flexibility in the maximum criteria for the condensing water entering the source-side network.

Annual hourly heating and cooling demand analysis of the building’s demand can readily identify if geo-exchange balancing would work with a reverse-cycle heat pump serving the whole demand – or if hybrid sources of heating or cooling are required. So it must be recognized that different seasonal performance factors (SPF) apply to heat pumping in winter and chiller operation in summer. The work of vapour compression in a heat pump combines with the heat extracted from the source-side network towards satisfying the building load with low investment. In contrast, the

work in chiller operation combines with the building demand to increase the heat-rejection load into the source-side network. For example, if the heat-pumping SPF_h is 4 while cooling SFP_c is only 2, then an entirely geo-exchange balanced installation (extraction=injection) would be achievable if the annual building heating loads (SPF_h-1) equal the annual cooling loads (SPF_c+1).

Some imbalances can be mitigated by oversizing the geo-exchange system, confirmed with long-term simulation to ensure that energy withdrawals and deposits find an equilibrium with excess heat or cold dissipating to the ambient. It appears that basement foundation diaphragm wall heat exchangers may provide a reasonable amount of buffering seasonal heating-cooling imbalance when underground carpark or tunnel ventilation systems are drawing ambient air to maintain air-quality.

Ideally the geo-exchange source-side network of foundation heat exchangers, thermal piles, and/or U-tubes in boreholes serves the annual demand for heat extraction, balanced by a comparable annual demand of heat rejection. It is important to note that by oversizing either the heat pump or chiller, then the overall seasonal performance is diminished. For the present study we have assumed that reverse-cycle heat pump/chiller equipment would be chosen based on the greater of the two building loads, with priority to charge the heating water accumulator before charging the chilled water accumulator. Generally superior seasonal performance would be expected if separate dedicated heat pumps and chiller were installed to specifically serve these building loads, which often are presented simultaneously.

In this case, the geo-exchange heat pump system supplies all the heating demand but only part of the cooling demand while air-source systems provide the remainder. The additional cooling demand may be met by installation of an additional heating, ventilation, and air conditioning system (HVAC) with rooftop air-coolers. Figure 1 illustrates reverse-cycle plant packaging, while Figure 3 illustrates how the operational components were represented in the course of the simulation methodology, with separate chiller and heat pump each able to simultaneously meet demands.

2. Methods

The analysis is based on validated DWHE installation in the Mediterranean climate of Barcelona, Spain[40, 47]. These walls are in contact with 1.6 W/m·K soil while inside are two levels of underground carparking with mechanical exhaust systems to maintain ambient air quality. For the current simulation study, it was assumed heat exchange pipework is included within basement retaining walls, and that these pipes also extend deep into foundation footings. Consequently, the default geometry provides for only 55% of diaphragm wall heat exchanger pipework below the basement floor (6.5 m_v/14.6 m_v). Another 45% (8.1 m_v/ 14.6 m_v) continues up to outdoor ground level with the retaining wall portion of the diaphragm walls. The advantage of the default geometry is that nearly half of vertical pipe length is in close contact with damp basement air that closely approaches outdoor ambient wet-bulb conditions.

FHX capacity must consider both heating and cooling conditions, and peak heat transfer and long-term demand, by undertaking a transient analysis of the assumed geoexchange schematic (Figure 3), using TRNSYS 17 Simulation Studio, TESS Libraries, and Rees' FHX dynamic module [1, 50].

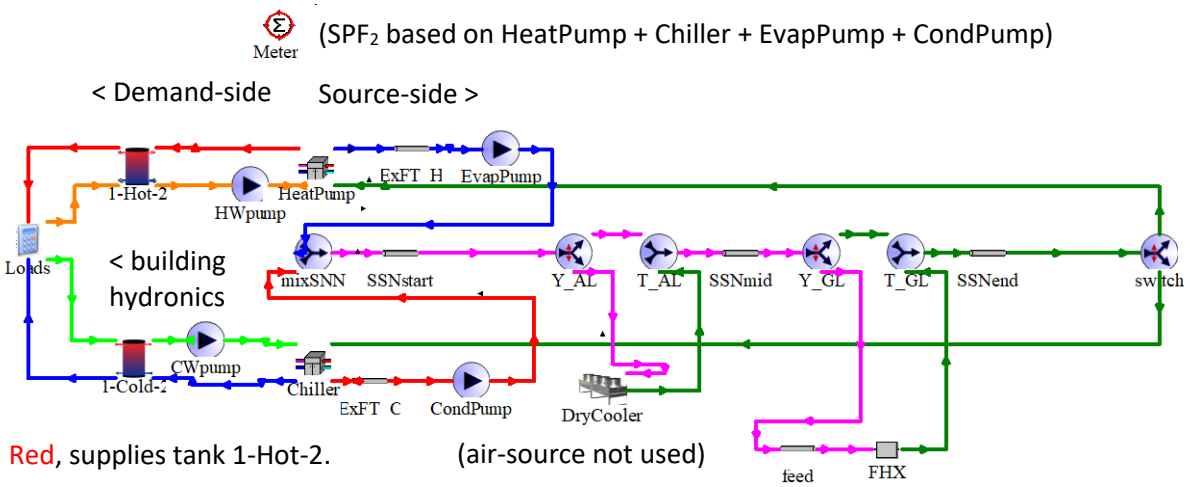

Red, supplies tank 1-Hot-2.

Orange, return to heat-pump condenser.

Light-green, return to chiller evaporator.

Blue, chilled water supply bottom of tank 1-Cold-2.

Blue pipe, conveys cold water leaving heat-pump evaporator.

Red pipe, conveys hot water from chiller condenser.

Green, outflow of either air- or ground-source heat exchangers returning to heat pump evaporator and chiller condenser.

Purple pipe, entering either DryCooler or FHX, which extract warmth or coolth as required.

Figure 3. Geoexchange system, with building demand-side on the left of heat-pump and chiller, and source-side confluence of water circuits through the heat pump evaporator and chiller condenser. Reject streams of heat-pump and chiller may run alternatively or blended simultaneously at "mixSSN". Source-side allows hybrid control with air-source DryCooler - not considered at present.

In the present study 20 years of flow of heat fluxes throughout the geoexchange system are simulated, using IWEC weather data [51] from nine European cities with the same building floor plan. System performance in each case with n=1, 2, ⋯ ,40 FHX modules were incrementally assessed to determine the minimum number of the DWHE type that would be necessary to sustainably maintain foundations between 1° and 37.8°C.

The model allows for hybrid air-cooled geoexchange system, but in the present paper all flow is fixed through ground FHX circuits rather than the Air Cooler (Figure 3). Red pipework on the demand-side represents hydronic heating water leaving the heat pump condenser and passing through the top of the stratified 1-Hot-2 accumulator to the building load. Blue pipework on the demand-side represents chilled water leaving the chiller evaporator and passing through the bottom of the stratified 1-Cold-2 accumulator to be delivered to the building Loads. Blue pipework on the source-side denotes water leaving the heat pump evaporator. Red pipework on the source-side denotes water leaving the chiller condenser. Purple pipework represents the source-side blend of condensing water from the chiller and evaporator water from the heat pump. The source-side pipework adopts a green colour after treatment in the DryCooler (air-source) or the FHX (ground-source) and is returned to the Chiller condenser or Heat Pump evaporator. Note air-source cooling via the DryCooler is not considered in the present paper but is readily simulated with these methods by various possible control schemes.

The grounded FHX component was developed at the University of Leeds [50] for TRNSYS, the Transient System simulation studio developed by the University of Wisconsin [52]. This module (denoted Type 5100) has been integrated into the building heating and cooling model that has been developed in the present work (Figure 3). Regardless of the selection of either U-tube, thermal pile,

and/or diaphragm wall heat exchangers, appropriate dynamic thermal networks (DTNs) could be developed to represent time-dependent heat fluxes between three boundaries (i.e. – indoor, basement, outdoor – or – heat exchanger, basement, ground surface) temperatures by superposition of unit step changes at each node, adjusted by weighting functions – with results calculated two orders of magnitude faster than a full three dimensional model [53-55]. Rees' FHX module [50] employs such a DTN to represent diaphragm walls heat exchangers [56], and could be adapted to represent energy piles. In this approach, the g-function, T_b-T_g +q(t)/2πk_s, is calculated with finite difference models with results tabulated for various geometries and characteristic times to be used in operational simulations [57, 58]. The concept of g-function is employed in DTN methods to simplify the computation of the complex interactions occurring between the heat transfer areas of a ground source system. The g-function is a transfer function linking the total ground heat exchange rate and the average heat exchanger wall temperature [59]. By convolving a time varying heat load signal with the g-function, the evolution of heat exchanger fluid temperature can be predicted [60]. DTN models of pipe buried into soil backfilled against basement walls proved numerically efficient for modelling complex residential geometries [61]. DTN models of FHXs of the diaphragm wall geometry with pipework cast in concrete together with structural steel reinforcement of footings (our prototype DWHE) was validated in a multi-storey commercial development [1, 47], and have been applied in previous works [56, 62].

The design of ground-source heat exchange systems to minimise life-cycle cost is complex and would be best achieved through a process of system simulation. In this project we have implemented a model of a diaphragm wall heat exchanger in the TRNSYS simulation environment to enable the optimal performance to be studied. This type of modelling seeks to represent individual components of the heating and cooling systems by their interconnections as illustrated in Figure 3, except that controls and output reporting have been supressed so the reader may better comprehend the major plant and pipework. Stratified chilled and hot water buffer tanks have been included to avoid short cycling of either the chiller or heat pump [63].

2.1. Method of control of geoexchange system as assumed during simulations

Many control strategies have been suggested for controlling geoexchange heat pumps systems. Geoexchange systems ideally should be include rudimentary artificial intelligence that forecast the seasonal impact of cyclic heat extractions and reinjections[29]. There are a wide variety of such control and modelling methods to potentially improve the inter-seasonal performance of ground coupled heat pump systems, such as vector and neural networks [11, 26], adaptive neuro-fuzzy interface [28], statistical weighting [29], fuzzy logic [30]. Such are beyond the scope of the present investigation, which employs simple reactive controls in response to intermittent demand of building services (Figure 3).

The following discussion assumes that building heating and cooling loads are delivered by hydronic hot and chilled water systems driven by two-stage heat pump/chillers with pumped water circuits on both the evaporator and condenser sides of vapour-compression equipment. We assume that chilled water is pumped from the bottom of cold buffer tank that is reactively recharged by a dedicated chiller. Similarly, we assume that hydronic heating water is pumped from the top of a hot buffer tank that is reactively charged by a dedicated heat pump. The nominal temperature rise on all water circuits are assumed to be 6-degree (Kelvin) delta-T, except this figure has been adjusted to maintain a constant 0.75 m/s water velocity through the foundation heat exchanger circuits.

This section outlines conventional control systems that were modelled in the process of designing foundation heat exchangers to match the heating and cooling loads of a prototypical office building in eight European cities. Four locations were heating-dominated while the other four were cooling-dominated. Heating and cooling loads to the building were modelled with separate hydronic hot and chilled water circuits pumped at a constant flow with a 6 Kelvin delta-T from dedicated stratified accumulator tanks sized with one-hour of capacity at design load. Design loads were taken as the 99.6% percentile of 8760 hours per year of simulated building demand for heating and cooling. This approach was aspiring for “right sizing” to achieve better energy performance during

typical operational hours of part load. Conventional reverse cycle heat pump/chiller operation was imposed by up-specifying the smaller of design heating and cooling capacities to equal the other and to interlock performance so that heating is satisfied before cooling. This assumption would not be necessary if separate dedicated heat pumps and chillers shared a common source-side network.

Chilled water supply to the building rises from the bottom of the cold accumulator tank (nominally 6 °C, blue pipework in Figure 3), while water returns to the chiller's evaporator via the top of the accumulator tank is illustrated 1-Cold-2 (nominally 12°C, green pipework in Figure 3). The first stage of chiller operation is enabled when temperature at the top of the tank rises above 6½°C, and continues until the temperature at the top of the tank sinks to 5½°C. The second stage of chiller operation is enabled when the temperature at the top of the tank rises above 7½°C and continues until it sinks back to 6½°C.

Hydronic hot water supply to the building comes from the top of the hot accumulator tank (nominally 35 °C, red pipework in Figure 3), while water returns to the heat pump's condenser via the bottom of the hot accumulator tank is illustrated 1-Hot-2 (nominally 29°C, orange pipes in Figure 3). The first stage of heat pump operation is triggered when temperature at the bottom of the hot water tank sinks below 34½°C, and continues until the temperature at the bottom of the hot water tank rises above 35½°C. The second stage of heat pump operation is triggered when temperature at the bottom of the hot water tank falls below 33½°C and continues until it returns above 34½°C.

The source-side of a geoexchange system heat pump's evaporator pump must not drop below 1°C, and may join a confluence "Y" fitting from a chiller's condenser pump . These two streams switch (or they may blend concurrently) to enter the source-side network (SSN) upstream of treatment are colour coded as purple pipework, while green pipework denotes water that has been charged with warmth or coolth, to return to chiller condenser and/or the heat pump evaporator.

In order to control foundation heat exchanger circuit velocities, it is necessary to adjust above or below the condensing-water rise that would be conventional practice in selecting air-

coolers for the source-side. A fixed ratio was found to hold constantly in proportion to the greater of the heat pump and chiller demand-side capacities, Q_{cap} and inversely proportional to the product of three factors: cross-sectional area of each pipe, $¼\pi\phi_{in}^2$, velocity v_{circ}. and number of circuits n_{FHX}.

$$\Delta T_{SSN} = \frac{298.93 \times Q_{cap}}{\frac{\pi}{4} \times \phi_{in}{}^2 \times v_{circ} \times n_{circ}} \quad (1)$$

As the heat pump and chiller are assumed to be a unitary package in the present study, there would be only one pump on the source-side network. Thus, the evaporator and condenser pumps were fixed to be equal sized, and operated in turns – resulting in a few unmet hours of service. Here, we focused on optimizing the use of foundation heat exchangers, the single source-side network pump has been modelled with a single speed of full-power operation to maintain foundation heat exchanger velocity v_{circ} at 0.75 m/s whenever either stage of either heating or cooling were called to recharge the hydronic hot water or chilled water accumulators on the demand-side.

2.2. DWHE dynamic thermal network files

A DTN model of a DWHE module [47,61] was employed to create the collection of time-dependent heat fluxes required in the Type 5100 module implemented in TRNSYS. The parameters used in the model to create the DTN files are detailed in Table 2. It was found necessary to increase the thermal conductivity of concrete to account for steel reinforcement as well as the conductivity of soil due to constant immersion in groundwater (~5 m_v below ground surface) [47,61]. Although the DTN DWHE model is based on vertical arrangement of pipes in the diaphragm wall, it has been shown to provide accurate data for both vertical and horizontal pipe layout. For horizontal pipe arrangement recalculation of pipe spacing and depth based on the wall size and number of loops is required. Five DTN files were created to match the DEFAULT geometry of the present paper, in accordance with five variations of soil – very low conductivity (0.9 W/m·K), moderately low conductivity (1.25 W/m·K), normal soil conductivity (1.6 W/m·K), moderately high conductivity (1.9

W/m·K), and very high conductivity (2.2 W/m·K), – while other properties are summarized in Table 2. Unless otherwise noted, 1.6 W/m·K soil conductivity is assumed in the present research, as was determined in the validation study [1, 47].

Table 2. DTN model of a DWHE module – parameters used for the DEFAULT geometry.

Property	Value	Unit
$Thickness_{wall}$	0.60	m_h
Cover	70	mm_h
$Depth_{wall}$	17	m_v
$Thickness_{basementslab}$	1.2	m_v
$k_{concrete}$†	2.25	W/m·K †
$capacity_{concrete}$	3.5	MJ/m^3K
PipeSpacing	0.40	m_h *
pipe, $Ø_{out}$	25	mm *,§
$Depth_{basement}$	6.5	m_v
$Depth_{pipe}$	14.6	m_v *
k_{ground}(nominal ‡)	1.6	W/m·K
$capacity_{ground}$	1.6	MJ/m^3K

*PipeSpacing, outside diameter $Ø_{out}$, and $Depth_{pipe}$ match TRNSYS Type 5100 (Table 4).
§ Pipe inner diameter $Ø_{in}$=0.81875 × $Ø_{out}$, according to DIN 16893 PE-Xa series 5 [64].
† Validation study confirmed the high end of material sample test results (1.9 to 2.5 W/m·K) [1, 47]
‡Also very low, moderately low, moderately high, and very high variations of k_{ground}.

The DTN model of a DWHE module (Table 2) was validated against data from walls where the main heat transfer area of the wall was located below the basement level where the pipe loops were accumulated as show in Figure 4. Their depth of active pipe coil below basement was 8.1 m_v ($Depth_{pipe}$ - $Depth_{basement}$), while DEFAULT geometry (Figure 5) would have more active heat exchanger cast into the available diaphragm walls, “pipe depth from the ground”. Since the DEFAULT geometry pipe depth below basement is also 8.1 m_v , the 6.5 m_v height of two levels of basement retaining walls increases the vertical length of active pipe, VL_{pipe} = 14.6 m. Thus 45% of active foundation heat exchanger coils are cast into retaining walls in contact with air.

This airspace represents two levels of underground car parking with pollutant exhaust extraction system acting as a hybrid air-source system without the capital expense of cooling towers. Consequently, the DEFAULT geometry can partially provide passive hybrid air-source cooling. The DEFAULT diaphragm wall heat exchanger geometry has been assumed throughout this research with 14.6 m_v VL_{pipe} casting 6 verticals per FHX circuit, with pipe spacing of 40 cm (Table 4 inputs) –

consequently each diaphragm wall module is 2.4 m_h wide and has an active area of 35 m² of which 15.6 m² is earth retaining wall above the lowest basement floor level.

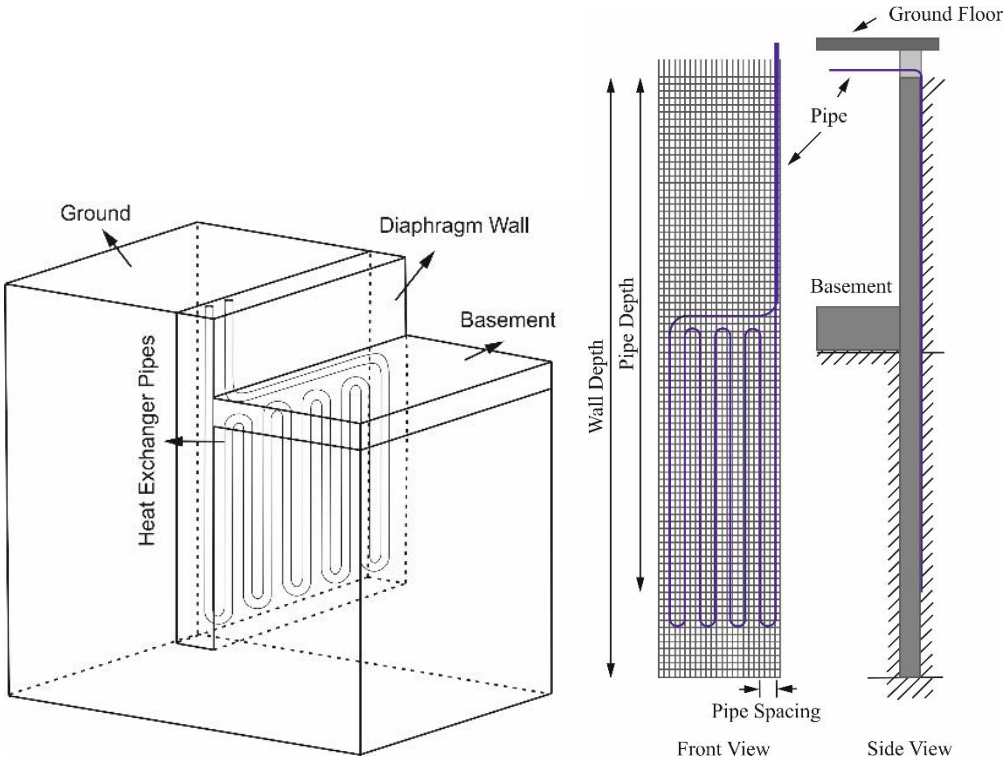

Figure 4. Diaphragm wall heat exchanger with pipes fitted below the basement level [65].

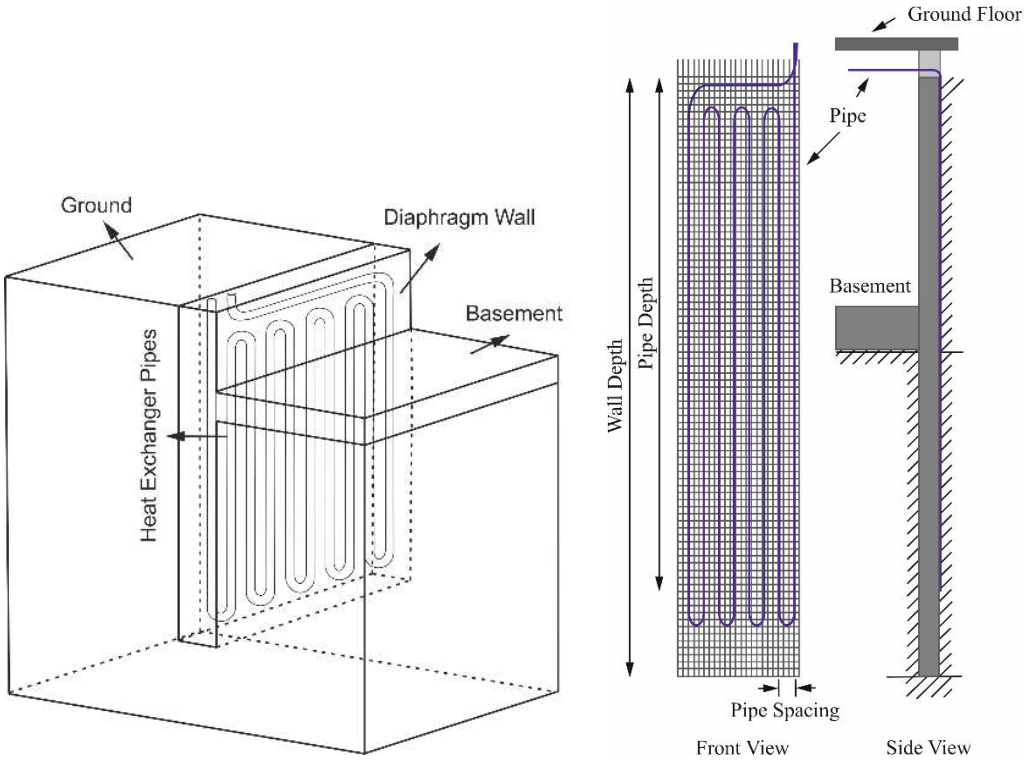

Figure 5. Pipe depth from the ground surface (DEFAULT) diaphragm wall heat exchanger [65] .

In summary, ground and concrete material properties from the foundation heat exchanger validation study [1, 47] were applied in our DEFAULT diaphragm wall heat exchanger – except different DTN files were required to distinguish the three-dimensional convolutions of thermal resistance underground. The assumed foundation heat exchanger geometry was then consistently applied in various European climates and soil properties with the assumed prototypical office building loads.

2.3. Prototypical Office Building Loads

Hourly heating and cooling loads of one floor of a 900m² open-plan office building with north, east, south, west, and core zones were modelled separately in various climates. The typical floor plan was 30 m_h × 30 m_h, which was assessed for simultaneous heating and cooling as required to maintain productive work environment given a weather file. Available foundation diaphragm wall length 120 m_h = 4 façades × 30 m_h, so fifty is the maximum number of DEFAULT geometry (2.4 m_h wide) DWHE modules that can be activated therein (n=50).

Annual 17,500 half-hourly loads for air-conditioning, heating, and service hot water were simulated on the basis of IWEC [51] climate data at nine locations: Barcelona, Paris, Amsterdam, Madrid, Athens, Nancy, Helsinki, Rome, and London. This was done in IESVE software. Note these loads exclude heat exchange between adjoining levels above and below. Consequently, the ground floor and the highest level require additional heat and cooling capacity. Figure 7 compares the building's partial-loading of heating and cooling at the 3 Mediterranean and 3 Oceanic sites. This is referred to as the 'prototypical' office building in this paper. One can multiply the loads depending on the number of floors. It transpired that the winter heating loads from Helsinki were so extreme that the ground source heat exchange system would freeze, and so it is suggested that Passive-Haus construction standards could reduce envelope R-values and ventilation air energy recovery, but such was beyond the scope of the current research. Feasible results became available (Table 3) for eight

load profiles (per floor), half moderately cool climates with Oceanic influences and half warmer climates with Mediterranean influences.

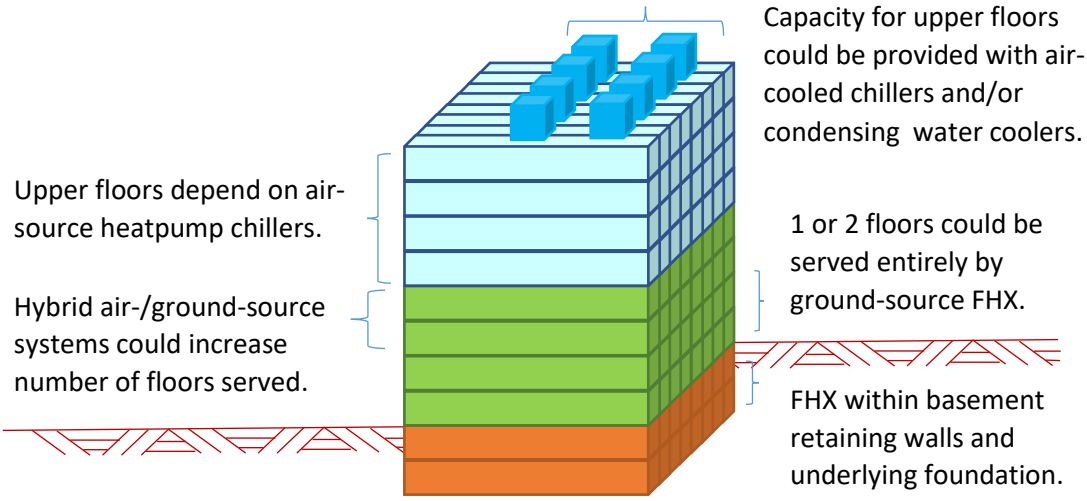

Figure 6: Prototypical office building. Two levels of underground carpark (brown) diaphragm wall foundation heat exchangers (FHX) are assumed. Above ground level (green) denotes replicated office floors which might be served by reverse-cycle ground-source heat pumps served by the limited FHX availability. Higher levels (blue) denote additional office levels which would require hybrid air-coolers to supplement FHXs, district cooling, or rooftop air-cooled chillers.

Table 3. Prototypical Office heating and cooling loads per floor (900 m²), warm Mediterranean (Csa) above double line, cool Oceanic (Cfb), and cold humid continental climate (Dfb) below triple line.

location	cool (GJ_a)	chiller kW	load factor	heat (GJ_a)	Heat pump kW	load factor	Nominal count DWHE/floor
Madrid (Csa>Bsk)	154	56	9%	22	11	1%	n = 25
Barcelona (Csa)	177	56	10%	33	6	2%	n = 27
Rome (Csa)	186	61	10%	34	7	2%	n = 30
Athens (Csa)	212	64	10%	33	7	2%	n = 29
Amsterdam (Cfb)	78	39	6%	52	24	4%	n = 23
London (Cfb)	71	29	8%	50	24	6%	n = 19
Paris (Cfb)	99	39	8%	54	26	4%	n = 21
Nancy (Cfb>Dfb)	92	38	8%	59	31	5%	n = 40
Helsinki (Dfb)	59	36	4%	134	49	9%	*
* n > 40 needed in Helsinki, but only if glycol concentration is sufficient for -7.5 °C							
DEFAULT DWHE modules are 2.4 m_h wide. Nominal soil conductivity 1.6 W/m·K.							

Table 4. TRNSYS Type 5100 diaphragm wall FHX

Model parameters	dimensions	nominal value
Pipe inner diameter, $Ø_{in}$	mm [0.0;+Inf]	20.5
Pipe outer diameter, $Ø_{out}$	mm [0.0;+Inf]	25
Pipe thermal conductivity	W/m.K [0.0;+Inf]	0.39
Pipe horizontal spacing	m_h [0.0;+Inf]	0.4
Pipe vertical length	m_v [0.0;+Inf]	14.6
Number of circuits, n	- [1;+Inf]	1, 2, 3,…, 40
Pipe sections per circuit	- [1;+Inf]	6
Circuit length	m_p [0.0;+Inf]	87.6
Fluid conductivity	W/m.K [0.0;+Inf]	0.625
Fluid specific heat	J/kg.K [0.0;+Inf]	4178
Fluid density	kg/m^3 [0.0;+Inf]	994
Fluid viscosity MU	Pa-s [0.0;+Inf]	0.000715
Shading factor	- [0;+Inf]	0
Initialization temperature	C [-Inf;+Inf]	20
DTN data unit number	any [0;+Inf]	1
Heat exchanger type	1 = wall, 2 = pile	1

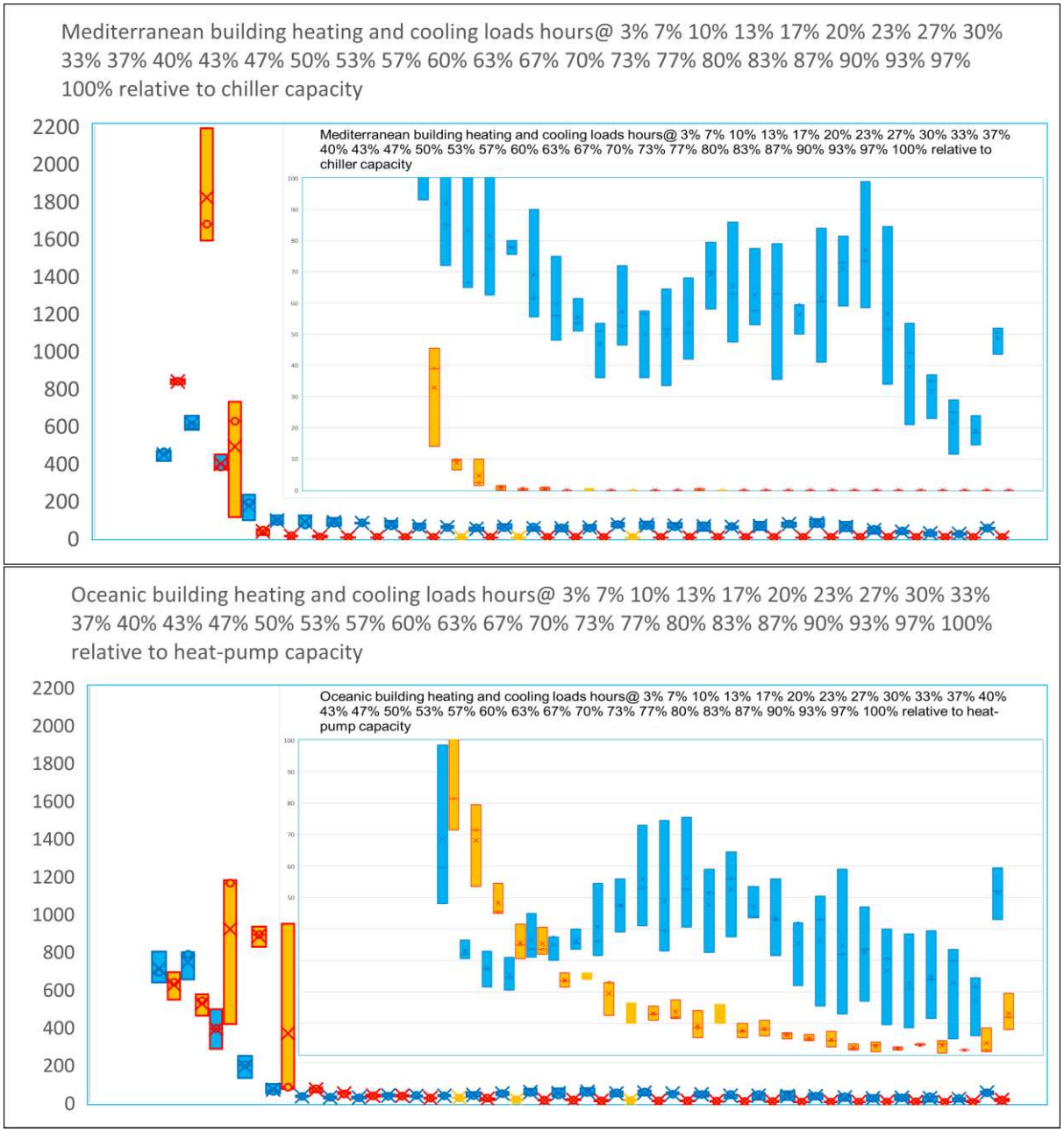

Figure 7. Part-load histograms from Mediterranean sites (upper pane) and Oceanic sites (lower pane) for the same prototypical office building floorplan. The range of heat-pump/chiller capacity was divided into 30 bins plotted across the horizontal axis. Frequency of hourly part-load occurrences is plotted in the vertical axis, where blue denotes cooling and orange denotes heating. The insets have vertical scale zoomed to 100 hours per annum, to resolve high loading. Boxes span between minimum and maximum, circles contain median, and crosses mark average of 3 values.

2.4. Integrating Type 5100 FHX with established TRNSYS objects

Simulation of foundation heat exchangers with TRNSYS 17 depended on the development of the Type 5100 module and the library of DTN files produced. The current research used Thermal Energy System Specialists (TESS) Libraries for many other system modules. TRNSYS Type 5100 diaphragm wall foundation heat exchanger nominal values must be initiated for all the parameter values (Table 4). Energy outputs from the type 5100 module are expressed in units of Watts and mass flow in kg per second, and so the user should multiply by 3.6 to convert into standard TRNSYS components with units of kJ/hour and kg/hour. Such operations may be made in the graphical simulation studio using calculator icons, or in command-line parametric studies within scripted deckfiles. Equations presented in this paper are used in the governing deckfile developed for this research.

Both the chilled water and hydronic hot water accumulator tanks serving building loads were sized to provide one hour of building demand with a delta-T of 6 degrees Kelvin. TESS Type 534 Stratified cylindrical storage tanks were used denoted in Figure 3 as 1-Cold-2 and 1-Hot-2.

WaterFurness™ performance data included with TESS libraries were the assumed performance data for Type 1221 water-water reverse cycle heat pump/chiller. Type 1221 is provided in TESS libraries as generic water-to-water 2-stage heat pump. Type 1221 is based upon WaterFurnace model EW540 catalogue normalization at 32°C source and 10°C load both 8.5 L/s.

Two separate type 1221 units were modelled concurrently – one as a dedicated chiller; and the other as a dedicated heat pump serving hydronic and service hot water to meet building loads. They were interlocked so that the hydronic hot water accumulator tank was satisfied by the heat-pump before the chiller was responsive to calls to charge the chilled water accumulator tank. The greater of either the chiller or heat-pump kW capacity (Table 3) was applied equally to both type 1221 units as Q_{cap}*, which is multiplied by 3600 to express the heat pump and chiller capacity in kJ/hr Q_{HP} and Q_{CH}. Based on WaterFurness™ EW540 data referred to by the TESS Library,

$Q_{HP,part}/Q_{CH,part}$, the partial capacity of the heat-pump/chiller is 50/52.5% respectively for heating/cooling modes. Similarly, $E_{HP,part}/E_{CH,part}$, the partial electricity demand of the heat-pump/chiller is 51/51.4% respectively for heating/cooling modes. COP of the WaterFurness is 4, so E_{HP} and E_{CH} were fixed the full electricity demand to be each one quarter of the respective heating and cooling capacity of the water/water package. Source-side pumping demand was accounted for to calculate SPF_2, assuming that E_{Evap} / E_{Cond} pump motor capacity is 1% of the specified plant heating/cooling capacity of the heat-pump/chiller, Q_{HP}/Q_{CH} [kJ/h]. The mass flow rates [kg/h] were calculated from the heat fluxes [kJ/h] according to equations 2-7:

Partial hot water production, $$\dot{m}_{HW,part} = {Q_{HP,part}}\Big/{C_p \Delta T_{nom}} \quad (2)$$

Full hot water production, $$\dot{m}_{HW} = {Q_{HP}}\Big/{C_p \Delta T_{nom}} \quad (3)$$

Partial chilled water production, $$\dot{m}_{CW,part} = {Q_{CH,part}}\Big/{C_p \Delta T_{nom}} \quad (4)$$

Full chilled water production, $$\dot{m}_{CW} = {Q_{CH}}\Big/{C_p \Delta T_{nom}} \quad (5)$$

Condenser flow to ground-source, $$\dot{m}_{cond} = {(Q_{CH} + E_{ch})}\Big/{C_p \Delta T_{FHX}} \quad (6)$$

Evaporator flow to ground-source, $$\dot{m}_{evap} = {(Q_{HP} - E_{HP})}\Big/{C_p \Delta T_{FHX}} \quad (7)$$

Supply-return thermal energy delivery depends on a temperature difference (ΔT). For demand-side circulation of chilled water and hydronic heating, as well as air-source condensing water the nominal delta-T (ΔT_{nom}) was set to 6 Kelvin. Hydronic hot water buffer tank charged to 35°C, returning 29°C at full load. Chilled water buffer tank charged to 6°C, returning 12°C at full load.

Source-side delta-T (ΔT_{FHX}) cannot be assumed to operate at such a constant differential. Ground-source foundation heat exchanger flow of either evaporator or condenser water the actual source-side delta-T (ΔT_{FHX}) generally needs to be varied from the nominal 6 Kelvin rule-of-thumb.

Variable ΔT_{FHX} proved necessary in order to regulate heat exchanger circuit flow at v_{circ} = 0.75 m/s. This is necessary to assure a consistent Reynolds number to achieve a balance of reasonable heat transfer without excessive head loss.

The forgoing imposed the form of equation 1 ΔT_{SSN} at the start of section 2.1. Consequently, the chiller condensing water pump must be variable speed driven at two speeds – *partial* and *full* – as the Type 1221 chillers/heat-pump requires such. So, a linear power demand is proportional to Gamma control signal that is either 0, partial, or 1. Following on, the source-side network pumping requirement for ground-source and air-source, and $\dot{m}_{FHX}$ is what pump size will accommodate both, is established as the greater of $\dot{m}_{EVAP}$, and $\dot{m}_{COND}$. Q_{ssn}, source-side network load expressed in kW load is from the heat-pump/chiller capacity and electric demand that was given in units of kJ/hr:

$$Q_{ssn} = (Q_{cap}* - E_{HP}/[3600\ s/hr] + Q_{cap}* + E_{CH}/[3600\ s/hr]) \quad (8)$$

$$Q_{ssn}* = \text{maximum}[\ (Q_{HP} - E_{HP})\ ,\ (Q_{CH} + E_{CH})\ ] \quad (9)$$

The asterisk in Q_{ssn}* denotes the source-side network design capacity for a unitary reverse-cycle heat-pump/chiller in units of kJ/hr. A 1% guideline for estimating pump motor E_{ssn} sizing in the units of kJ/hr (required for TRNSYS) was applied, based on source-side-network duty.

$$E_{ssn} = Q_{ssn}* \times 1\% \times (\Delta T_{nom} / \Delta T) \quad (10)$$

3. Results

3.1. Individual simulations

Each of the tabulated recommendations depended on a sequence of 40 simulation – incrementing the number of FHX modules from one to 40 – for each specified combination of climate data, heat/cool load profile, and soil conductivity. Thereby the lowest number *n* of FHX modules that achieved an acceptable solution in 20 years of hourly simulations are reported here. The most important criteria is to never experience evaporator water temperature within one degree

above zero, in addition to ensuring that condensing water temperature never exceeded 37.8°C (human fever temperature).

Table 5 shows the results of only two of 40 simulations that were provided to establish the threshold of acceptable operation for nominal soil conductivity (1.6 W/m·K), and another two of 40 simulations that were necessary in order to establish the summary for the next lower tier of soil conductivity (1.25 W/m·K). The moderate reduction of soil conductivity results in rising condensing temperature rise to a maximum of 47.8°C with n=21 FHX modules. In case of moderately reduced soil conductivity for the given building loads in Barcelona, then n=27 circuits that would be required to prevent exceedance of 37.8°C maximum during 20 years of operation as a geoexchange system.

Figure 8 illustrates the nominal soil conductivity case with the full recommendation of n=27 (f_{FHX}=100%), compared the impact of having only n=18 FHX circuits (f_{FHX}=67%). The third bar in either of the two panes of Figure 8 represents comparable energy recovery within the source-side network in the process of blending water leaving the chiller condensing and heat pump evaporator. Since these simulations assume continuous geoexchange operation, there is no fan energy nor heat rejection through air-coolers. Consequently (black bars), the source side is entirely ground-source provided by pumping energy, and there is no air-source nor fan energy demand – which would be denoted with golden coloured bars in case hybrid air-source operations had been simulated. Useful heat-pump compressor work makes a small contribution to the building heating load denoted by red bar below the black in the right most column of either case. The blue and red bars in the third column of either case demonstrates the substantial contribution of energy recovery within the source-side network by blending the exhaust of heatpump evaporator and the chiller condenser during shoulder seasons of the year – when the building is demanding both heating and cooling simultaneously.

Table 5: Barcelona DEFAULT FHX performance degradation with variation of the fraction (f_{FHX}) of the nominated number (n=27) of foundation heat exchangers (FHX). Upper two rows compare nominal soil conductivity with lower two rows moderately reduced soil conductivity (22% lower than nominal).

	FHX perimeter	n=27 f_{FHX}	bidecadal ΔT/20 y	min evap.	max cond.	SSN design	ΔT_{FHX}	SSN pump kW	SSN pump work	Heat pump	Chiller	SPF_2	unmet hours/year
nominal soil conductivity (1.6 W/m·K)													
n=27 †	65 m_h	100%	-0.9°C	8.4°C	37.3°C	6.7 kg/s	2.5°C	1.67	11 a.GJ	12 a.GJ	42 a.GJ	3.66	84
n=18 ‡	43 m_h	67%	-0.5°C	7.6°C	**47.1°C**	4.4 kg/s	3.8°C	1.11	8 a.GJ	12 a.GJ	45 a.GJ	3.69	96
moderately reduced soil conductivity (1.25 W/m·K)													
n=32†	77 m_h	119%	-0.9°C	9.6°C	37.6°C	7.9 kg/s	2.1°C	1.98	14 a.GJ	12 a.GJ	42 a.GJ	3.52	85
n=21 ‡	50 m_h	78%	-0.4°C	9.2°C	**47.8°C**	5.2 kg/s	3.2°C	1.30	9 a.GJ	12 a.GJ	46 a.GJ	3.59	91

Daggers † are cases where the design criteria were fixed at 37.8 °C maximum condensing water. Double daggers ‡ condensing guideline raised to 47.8 °C.

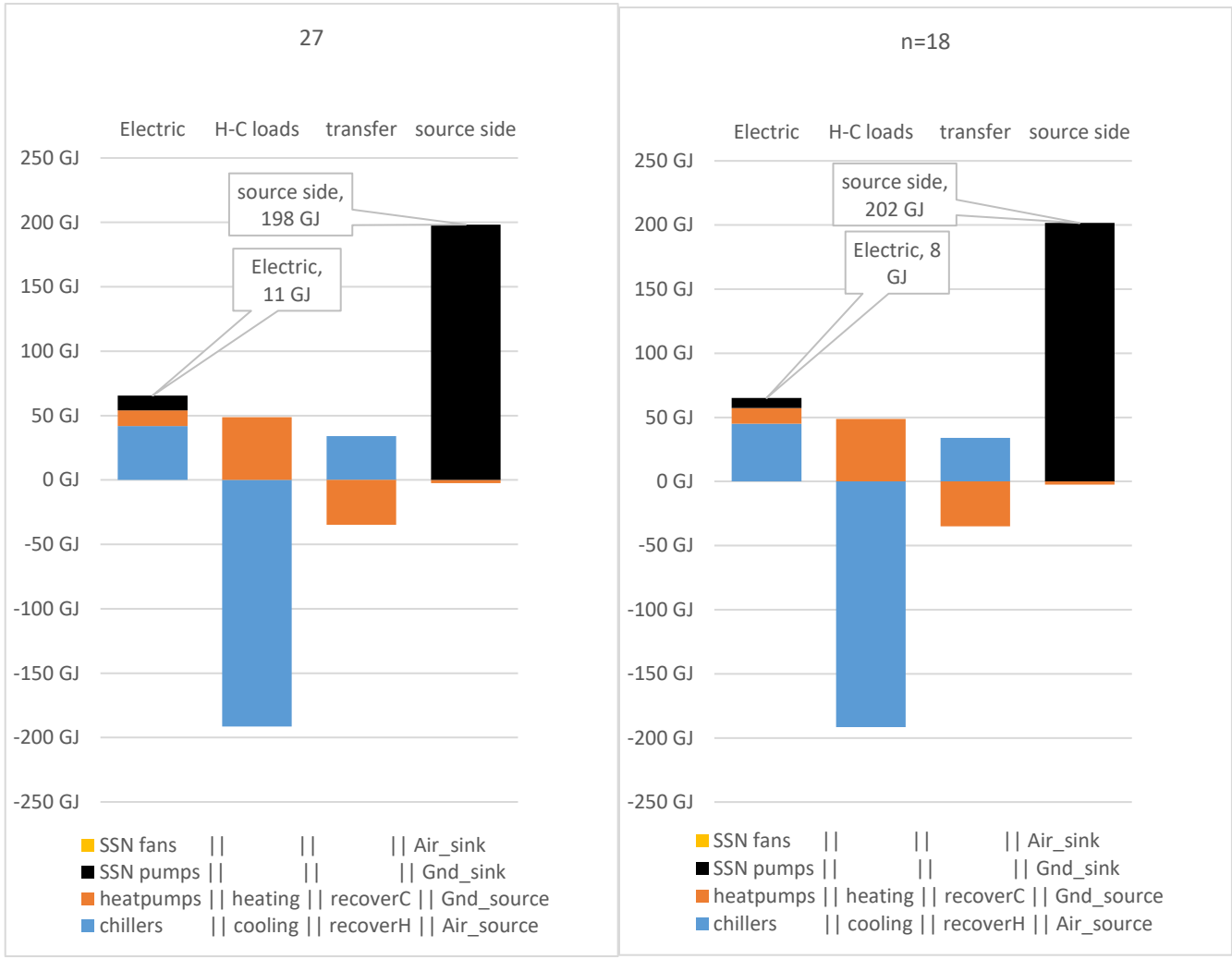

Figure 8. Barcelona example annual average simulation results with continuous heat injection and/or heat extraction through FHX circuits. Nominal soil conductivity (1.6 W/m·K). These plots present simulated annual energy metering without any air-cooling, entirely geo-exchange operation for 20 years.

3.2. Summary tables

Nominal results are in the right-most column of Table 3, where “Nominal FHX/floor” is the minimum number ***n*** of default geometry DWHEs. This was the simulation case that was found to serve 20 years without condensing water ever exceeding 37.8 °C, nor evaporator water descending below 1 °C. Since the perimeter length of the prototypical building plan accommodates up to n=50 parallel modules of the FHX, that divided by “Nominal FHX/floor” answers the question of how many stories can be served by geoexchange. Thus, perhaps three stories could be served in London, two stories in Madrid, Barcelona, Amsterdam and Paris, but only one story in Rome, Athens and Nancy. A more detailed approach is given in the discussion.

Repeated simulations were required to increment from n=1 to n=40 FHX circuits until a satisfactory solution was found and then only those results are reported herein. Peak and annual heat flux injection and extraction into/from the default diaphragm wall geometry for the prototypical building loads just inside the safe operating criteria are presented in Tables 5 for nominal soil conductivity. Sensitivity of results with respect to soil conductivity in presented in Table 7 (Mediterranean influenced climate) and Table 8 (Oceanic influenced climate).

Tables 7 and 8 summarise DWHE potential for a prototypical office building in four warm and four colder climate locations, each with a range of different values of ground thermal conductivity. All assumed non-hybrid operation, without ever diverting flow through an air-cooler. The pipe spacing is 400mm, pipe size 25mm and active length 14.6m.

The limiting criteria in warm continental Madrid as well as Mediterranean Barcelona, Rome and Athens is to establish allowable heat rejection (highlighted in red) to prevent condensing water temperatures from exceeding 37.8 °C, therefor there is undetermined scope to increase heat extraction during winter unless measures are taken to reduce cooling load in summer. The limiting design criteria in cool oceanic Amsterdam, London, and Paris, and continental-influenced Nancy-Strasbourg is to establish allowable heat rejection (highlighted in blue) to prevent evaporator water

temperatures from falling below 1 °C, therefor there is undetermined scope to increase heat rejection during summer unless measures are taken to reduce heating load in winter. DWHE heat exchange potential for a prototypical office building in different locations. Here, the pipe spacing is 400mm, pipe size 25mm and active length 14.6m.

Table 6. Non-hybrid operation, entirely ground-source without any air-coolers or cooling towers. Ground thermal conductivity is 1.6 W/m·K. † and * denote locations with continental influences.

Non-Hybrid	**Performance per unit horizontal perimeter length of DEFAULT foundation diaphragm wall (45% basement aspect ratio**				**Performance 25 mm $Ø_{out}$ circuitry cast within DEFAULT foundation diaphragm wall per unit pipe length (45% basement aspect ratio**			
	heat extraction		heat rejection		heat extraction		heat rejection	
Location	peak W/m_h	annual MJ/m_h	peak W/m_h	annual MJ/m_h	peak W/m_p	annual MJ/m_p	peak W/m_p	annual MJ/m_p
Madrid †	581	63	**1226**	**2937**	16	2	**34**	**80**
Barcelona	549	25	**1078**	**2999**	15	1	**30**	**82**
Rome	537	35	**1056**	**2863**	15	1	**29**	**78**
Athens	584	27	**1129**	**3421**	16	1	**31**	**94**
Amsterdam	**459**	**333**	918	1362	**13**	**9**	25	37
London	**395**	**377**	808	1479	**11**	**10**	22	41
Paris	**489**	**390**	956	1994	**13**	**11**	26	55
Nancy *	**249**	**242**	510	951	**7**	**7**	14	26
$flux/unit\ area$	Divide the above by 14.6 m_v VL_{pipe}				Divide the above by 0.4 m_h pipe spacing			

The resulting heat rejection (MJ/m or MJ/m²) per annum is primarily driven by climate and higher values correspond to locations with warmer Mediterranean climates. Conversely, higher annual heat extraction capacities correspond with cooler Oceanic climates. Geographic trends are not as strongly differentiated among peak heat transfer rates (W/m_h or W/m_p) as these represent the peak rate at one particular time of the year.

Table 7. DWHE potential for prototypical office building in warm climate locations. The limiting criteria was to establish allowable heat rejection to prevent condensing water temperatures from exceeding 37.8 °C, therefor there is undetermined scope to increase heat extraction during winter.

Location	Soil thermal conductivity W/m.K	Number of DWHE used (each 2.4m_h wide)	Performance per unit horizontal perimeter length of DEFAULT foundation diaphragm wall (45% basement aspect ratio)				Performance 25 mm $Ø_{out}$ circuitry cast within DEFAULT foundation diaphragm wall per unit pipe length (45% basement aspect ratio)			
			heat extraction		heat rejection		heat extraction		heat rejection	
			peak W/m_h	annual MJ/m_h	peak W/m_h	annual MJ/m_h	peak W/m_p	annual MJ/m_p	peak W/m_p	annual MJ/m_p
Madrid †	0.9	n=40	307	31	**730**	**1840**	8	1	**20**	**50**
	1.25	n=31	438	47	**1022**	**2365**	12	1	**28**	**65**
	1.6	n=25	584	63	**1226**	**2935**	16	2	**34**	**80**
	1.9	n=22	686	77	**1402**	**3343**	19	2	**38**	**92**
	2.2	n=22	686	79	**1416**	**3343**	19	2	**39**	**92**
Barcelona	0.9	n=40	312	9	**755**	**2030**	9	0	**21**	**56**
	1.25	n=32	439	16	**919**	**2531**	12	0	**25**	**69**
	1.6	n=27	549	25	**1078**	**2999**	15	1	**30**	**82**
	1.9	n=24	638	32	**1227**	**3374**	17	1	**34**	**92**
	2.2	n=24	636	35	**1226**	**3372**	17	1	**34**	**92**
Rome	0.9	n=36	423	25	**876**	**2380**	12	1	**24**	**65**
	1.25									
	1.6	n=30	540	35	**1051**	**2862**	15	1	**29**	**78**
	1.9									
	2.2	n=27	613	42	**1197**	**3183**	17	1	**33**	**87**
Athens	0.9	n=40	357	12	**793**	**2494**	10	0	**22**	**68**
	1.25	n=35	462	19	**911**	**2833**	13	1	**25**	**78**
	1.6	n=29	584	27	**1129**	**3421**	16	1	**31**	**94**
	1.9	n=26	676	34	**1273**	**3811**	19	1	**35**	**104**
	2.2	n=26	674	36	**1273**	**3805**	18	1	**35**	**104**
flux/unit area:			Divide the above by 14.6 m_v VL_{pipe}				Divide the above by 0.4 m_h spacing			

Mediterranean heat saturation (Table 7) highlights the significance of ground thermal conductivity as a design parameter and the importance of having a good estimate of its value at a project site. Bear in mind that presence of groundwater near the foundation tends to increase the thermal conductivity. Variations in the predicted heat transfer rates at three Oceanic locations and a range of five values of ground thermal conductivity (Table 8), are sub-optimal above and below the nominal 1.6 W/m·K. The general trend is that increasing values of ground thermal conductivity

improve performance. However, results for the highest values (2.2 W/m·K) show that increased interaction with the adjacent ground surface can limit the maximum performance. In the case of Oceanic climates (Table 8), high soil conductivity can lead to unacceptably low fluid temperatures, the heat exchange must be limited, especially in continentally influenced Nancy.

Table 8. DWHE potential for prototypical office building in four cool climate locations. The limiting criteria was to establish allowable heat rejection to prevent evaporator water temperatures from falling below 1 °C, therefor there is undetermined scope to increase heat rejection during summer.

Location	Soil thermal conductivity W/m.K	Number of DWHE used (each 2.4m_h wide)	Performance per unit horizontal perimeter length of DEFAULT foundation diaphragm wall (45% basement aspect ratio)				Performance 25 mm $Ø_{out}$ circuitry cast within DEFAULT foundation diaphragm wall per unit pipe length (45% basement aspect ratio)			
			heat extraction		heat rejection		heat extraction		heat rejection	
			peak W/m_h	annual MJ/m_h	peak W/m_h	annual MJ/m_h	peak W/m_p	annual MJ/m_p	peak W/m_p	annual MJ/m_p
Amsterdam	0.9	n=36	**248**	**196**	599	861	**7**	**5**	16	24
	1.25	n=23	**438**	**324**	920	1358	**12**	**9**	25	37
	1.6	n=23	**453**	**333**	920	1358	**12**	**9**	25	37
	1.9	n=23	**467**	**342**	949	1372	**13**	**9**	26	38
	2.2	n=37	**292**	**212**	599	847	**8**	**6**	16	23
London	0.9	n=30	**219**	**220**	496	920	**6**	**6**	14	25
	1.25	n=19	**380**	**366**	803	1475	**10**	**10**	22	40
	1.6	n=19	**394**	**377**	803	1475	**11**	**10**	22	40
	1.9	n=18	**438**	**407**	876	1562	**12**	**11**	24	43
	2.2	n=31	**248**	**237**	511	905	**7**	**6**	14	25
Paris	0.9	n=32	**307**	**239**	672	1299	**8**	**7**	18	36
	1.25	n=21	**467**	**381**	964	2000	**13**	**10**	26	55
	1.6	n=21	**482**	**390**	949	2000	**13**	**11**	26	55
	1.9	n=21	**496**	**399**	978	2000	**14**	**11**	27	55
	2.2	n=40	**263**	**207**	511	1037	**7**	**6**	14	28
Nancy *	0.9	n=38	**263**	**250**	540	993	**7**	**7**	15	27
	1.25	n=38	**263**	**250**	540	993	**7**	**7**	15	27
	1.6	n=40	**248**	**242**	511	949	**7**	**7**	14	26
	1.9	n=39	**263**	**253**	540	978	**7**	**7**	15	27
	2.2	n=39	**263**	**253**	540	978	**7**	**7**	15	27
***flux/unit area*:**			Divide the above by 14.6 m_v VL_{pipe}				Divide the above by 0.4 m_h			

3.3. Results in the context of previous research

To contextualise the contribution of the present results, literature review detailed in Table 1 includes peak and annual performance of Barcelona heat rejection and Amsterdam heat extraction results (Tables 6, 7, and 8). These peaks are the maximum half hour magnitude from 20 years' simulations and can be converted as noted at the foot of Tables 8 and 9 to flux per unit area to compare with others' common denominator of W/m².

As a nominal representative of heating load dominated oceanic climate (Cfb), Amsterdam simulations for 0.9 to 2.2 W/(m·K) soil conductivities had peak ground source rates 196 to 342 W/m², but the greater result was found in simulation with a less extreme soil conductivity of 1.9 W/(m·K). London and Paris simulations also resulted in lower DWHE capacity for 2.2 1.9 W/(m·K) soil conductivity. This is the result of disqualifying any simulation where evaporator temperature ever drops below 1°C. Others [38, 41] assumed basement walls were insulated on the intrados side, neglecting freezing risk in winter, while ignoring the benefit of cooling effect in summer due to parking exhaust air systems. Melbourne's climate is also Oceanic (Cfb) while 1.1 to 3.3 W/(m·K) soil conductivity were used in others' simulations [41]. Geneva's climate (Cfb) is also Oceanic, where another research group worked with 1 to 2.5 W/(m·K) soil conductivity [46]. Three other research teams' research was cast in humid subtropical climates (Cfa) with 2.8 W/(m·K) soil conductivity in Turin [38], 2.2 W/(m·K) in Milan [15], and 1.74 W/(m·K) in Shanghai [14]. Yet another team worked with 2.0 W/(m·K), and increasing with groundwater, in reference to the forementioned research cast in Cfa climates [14, 38], but no prior research on DWHE was found to be cast in situations with the Mediterranean climate (Csa).

As a nominal representative of cooling load dominated Mediterranean climate (Csa), Barcelona simulations for 0.9 to 2.2 W/(m·K) soil conductivities had peak ground source rates -52 to -84 W/m². These results are lower than others' initial thermal response tests (TRT) rates in Shanghai and

Geneva [3, 46] and parametric analysis of simulations [12], while higher than Torino summer peak performance [38].

The presented Barcelona results are higher than “realistic” asymmetric seasonal demands imposed on ground source heat exchangers (|heat pumping extraction| < |cooling heat rejection|) in Melbourne [41]. Divide Table 1 entry “-67 W/m_h“ by corresponding 20 m_v vertical height to compare -3.3 W/m² with others [12, 38, 46]. Note that the Melbourne simulations assumed basement walls were insulated on the intrados side, their simulation does not take into account heat transfer to the air [41]. In addition, it was not suggested that they included dynamic pulses of alternating heating and cooling loads that were imposed in the present simulations (Figures 7 and 8, Table 7).

Extended performances reported by others are more comparable with the present contribution, except the two-day TRT report of -48 W/m² at Shanghai Museum of Natural History [3] extrapolated to the annual equivalent -57,000 MJ_a/m_h is an unreasonable expectation. Table 1 shows that others [12, 15, 38, 41, 46] have provided much longer duration assessments of SWHE performance with geometry varying from 10 to 21.6 m_v vertical height of DWHE while their aspect ratio of basement to overall height ranges from 50 to 75%.

As the present results assume 45% basement aspect ratio within 14.6 m_v vertical, comparisons are not perfectly normalised by vertical area (W/m²). So, Table 1 also compares on the basis of the horizontal length of installed basement wall at the perimeter of buildings (W/m_h as well as MJ_a/m_h). The safe annual heat injection finding for Barcelona of about -5 W/m² is more conservative than all of the others. This is partially due to the lower basement aspect ratio of the Barcelona DWHE, but also probably due to the criteria not to exceed 37.8°C condensing water temperature, while others allowed higher operating temperatures. Results in Table 5 indicate that relaxation of these criteria increases heat transfer.

Results reported in the present work depend upon the building heating and cooling loads as well as DWHE geometry. It should be noted that differences between this research and other reported data

might be due to the fact that in the present research simulation results outside 1°C and 37.8°C DWHE fluid temperature are rejected. Also, the present results differ from the others [12, 15, 38, 41, 46] as we have included realistic building services loads of heating and cooling. To illustrate the differences between plausible Mediterranean and Oceanic part-load intermittency Figure 7 (Barcelona and Amsterdam) histograms show that full heating and cooling design loading is rare. The coincidence of heating and cooling loads in different zones of the prototypical building are evidenced by heat recovery "transfer" between heating and cooling zones in Barcelona. The effective energy recovery transfer was a consequence of the confluence of condensing water leaving the chiller and evaporator water leaving the heatpump. This mixed confluence or intermittent switching between heating and cooling (Figure 3) moderates the source-side duty of DWHEs.

4. **Discussion of the present results in terms of climate and the thermal conductivity of soil**

The present results include a range of climates while others [12, 15, 38, 41, 46] each only reported on one situation for their particular specifications of DWHE geometry. The present work has integrated our particular DWHE installed with a range of soil conductivities serving a prototypical building with heating and cooling loads from a range of climates. For each combination of climate and soil the number of DWHE modules was incrementally increased until the geoexchange system could be ensured to not freeze in winter, nor exceed 37.8°C in summer.

The range of results for sustainable extraction of heat in Amsterdam, and sustainable heat injection in Barcelona have been included in Table 1 to compare with previously published guidelines. Others' guidelines are not as conservative as the current findings, some of which focus on the enhanced opportunity of groundwater. The current paper's findings are of course dependent on the particular specification of lowest basement and foundation embedment below that level.

While the requirement not to freeze foundation heat exchangers is well established [12], the present work introduced an upper constraint for condensing water not to exceed human metabolic temperature (37.8 °C) entering diaphragm wall foundation heat exchangers. Table 5 indicates performance increases about 50% in Barcelona if the permitted threshold is raised 10 degrees.

The DEFAULT geometry assumes continuous ventilation is provided on one side of the upper 45% of SWHEs with outdoor and damp evaporative conditions are affecting a partially hybrid air-source dynamic such that conventional cooling towers or dry coolers might not be required if sufficient DWHE capacity is installed and activated. The dynamic thermal network methodology has been applied with the DEFAULT geometry described in the present paper that extends heat exchange through retaining walls that form two levels of underground carparking, ”pipe depth from the ground surface”.

The present work estimates the DEFAULT DWHE heat exchange potential for the same prototypical building plan if it were replicated in eight European cities of which 3 are Mediterranean, one warmer location with continental influences, 3 are Oceanic, and one cooler location with continental influences. Bi-decadal simulations showed that 30 W/m_p peak rejection per meter of heat exchanger pipework cast into foundation diaphragm walls at 400 mm spacing is sustainable without exceeding 37.8°C condensing temperature. In the Oceanic climate of Paris and Amsterdam simulations we found a limit of 13 W/m_p of peak heat extraction without freezing.

In Oceanic locations, foundation heat exchanger potential is limited by winter heat extraction, and so demand-side load reduction or supplemental heating will be needed if ground-source heat exchangers capacity is less than what we recommend. In Mediterranean locations foundation heat exchanger potential is limited by summer heat-rejection, and so hybrid air-source heat rejection capacity is suggested if ground-source heat exchanger capacity is less than the recommendations. Integration of heat-exchange pipework among the steel reinforcement before pouring concrete foundations generally benefits the seasonal performance of reverse-cycle heat

pump installations, but redundant air-source heat exchange will be required unless ground-source capacity is sufficient.

In addition to the geometric parameters noted in this paper (pipe size, spacing, active depth, and depth of basement) and the dynamic fluid flow conditions, the potential for heat exchange is strongly influenced by the ground thermal conductivity and atmospheric climate above ground. Initial calculations were conducted based on nominal 1.6 W/m·K soil thermal conductivity in Tables 6, 7 and 8 in a range of European climates. These have been calculated for a prototypical office floor-plan with heating and cooling load profiles. Values are reported per unit length (in the horizontal perimeter direction), and also per unit of serpentine circuitry pipework cast within basement diaphragm walls. Results have been calculated assuming all loads are met by diaphragm wall FHXs.

Varying soil conductivity in three Mediterranean locations were compared to the Spanish capital Madrid, as an example of warm continental influences (Table 7). Performance generally improves with increasing soil conductivity in these warm climates. Conversely designers should be concerned if water tables diminish, resulting in consequently lower soil thermal conductivity.

Varying soil conductivity in three Oceanic locations compared to Nancy is an example of cool continental influences near the European capital of Strasbourg (Table 8). Performance increases in cool ocean climates with a moderate increase soil conductivity of 1.9 W/m·K, but is lost if conductivity rises to 2.2 W/m·K – as required to prevent freezing of the FHX. Performance is hindered accross all soil conductivities in the continental-influenced French city of Nancy.

In the case of the cooler Oceanic (Cfb) climates of Paris, Amsterdam, London, and continentally-influenced Nancy (Cfb/Dfb), all available waste heat should be stored in the foundations and adjoining ground until winter when there is a need to extract and reuse this heat. In colder continental locations such as Helsinki (Dfb), substantially better demand-side management (building insulation) and supplemental heating could be afforded by rooftop photovoltaic panel connected to emersion elements added into the hydronic water accumulator tank but was beyond

the scope of the present campaign of parametric building simulation, and so we could not provide specific design guidelines.

In the case of climates where winter heating is a greater problem than summer cooling, a load-side recommendation is to improve building insulation standards – as required to maintain heat pump evaporator water always above 1°C. Ideally the FHX circuits are most effective if they are balanced to exploit as much as practical of the allowable range of 1°C to 37.8°C extremes of evaporator and condenser water temperature without ever exceeding these guidelines.

The practical application of the present paper has been seasonally balanced heat injection and extraction from the foundation walls of underground carpark basements of multi-story developments in a range of climates. Results show that our methods can answer a general question: what is the heat exchanger potential of such a foundation heat exchanger given its geometry, building load profile and ground conditions? Given a particular building floorplan and a range of European climates, the number of DWHE used (n) given in Tables 7 and 8 indicate how many stories could be served by a chiller/heat-pump system using the diaphragm walls and whether supplementary heat exchangers may be needed in a hybrid configuration. Thus, estimating with equation 11, almost three stories could be served in London, two stories in Madrid, Barcelona, Amsterdam and Paris. There appears to be capacity for *almost* two stories in Rome or Athens but only one story could be accommodated in Nancy unless the standards of building insulation were improved.

$$\text{Stories} = \text{Perimeter}_{\text{building}} / (\text{width}_{\text{DWHE}} \cdot n) = (120\ m_h/2.4\ m_h)/n = 50/n \qquad (11)$$

4.1. Condensing temperature will rise if the installed FHX capacity is insufficient (f_{FHX})

Consider a performance indicator denoted f_{FHX} defined by the ratio of available diaphragm wall circuitry divided by what is recommended on the basis of nominal soil conductivity (Table 6).

Then consider the possibility of allowing extreme condensing water temperatures to exceed the guideline of 37.8°C and thereby injecting more warmth in summer. In which case ground-source heat is more easily extracted in winter – with overall improvement of seasonal performance factor (SPF). The caveat of this operation is to understand the source-side network exceed the thermal guideline of human metabolic temperature, which could lead to unacceptable conditions in the area of the basement adjoining activated FHXs. High condensing temperatures result from low values of f_{FHX}, active foundation heat exchanger relative to recommendation for nominal soil (1.6 W/m·K). The high condensing temperature are not a fault of air-cooler selection – but are due to the required foundation ΔT_{FHX} (equation 1) necessary to maintain a fixed circuit velocity (nominally 0.75 m/s).

Table 5 presents detailed results from simulations of Barcelona DEFAULT geometry for the base case of normal nominal soil conductivity (1.6 W/m·K), and also for marginally reduced soil conductivity (1.25 W/m·K). The number **n** refers to the number of DEFAULT foundation heat exchanger circuits found to satisfy either 37.8°C (black) or 47.8°C (red) maximum temperature entering the source side network as well as the requirement to never drop below +1°C. As n=27 is the nominal soil recommendation to avoid exceedance of 37.8°C, the f_{FHX} is determined. The bidecadal ΔT is the 20-year trend of annual mean temperature of FHX circuitry. This is offered as surrogate for the rate of change of foundations. The “min evap” and “max cond” are the extremes in 20 years of the evaporator water and condensing water entering the source side network.

SSN design flow rate and delta-T are as required to maintain 0.75 m/s velocity within FHX circuitry. The annual electric energy use is presented for the source-side network pumps. The annual energy demand of the heat pump as well as chiller operation are presented with the overall seasonal performance factor of the reverse cycle heat pump combined with fans and pumps on the source side network, based on pump sizing at 1.5% of source side duty. SPF_2 does not consider the chilled water pumps, nor the hydronic hot water circulation pumps.

As an example of design application, consider prototypical building floor plan cooling load are 177 GJ per annum with a peak requirement of 56 kW in Barcelona (Table 4). Because heatpump COP is 4, the heat rejection into FHXs is 25% greater than the building cooling loads. Given 120 m_h building perimeter, the heat rejection load is 1475 MJ_a/m_h with a peak of 467 W/m_h. Factor in the 2999 annual-MJ/m with peak 1078 W/m_h (nominal ground-sourced rejection capacity from Table 6), and the number of repeated floors that could be served in Barcelona is barely two.

There would be 85% less performance in moderately reduced soil conductivity (1.25 W/m·K) in Barcelona. This is confirmed by the 85% ratio (n=27 / n=32) comparing the FHXs required for nominal soil conductivity to what is required for moderately reduced soil conductivity. Condensing water temperature could rise more than 5K with incremental reduction of soil conductivity (Table 5).

Other literature (Table 1) does not include analysis of how to avoid overheating foundations. Others' higher heat flux rates are reported per meter of pipe or per unit diaphragm wall area.

5. Conclusion

The present study extends design options for "geoexchange" systems – electrically powered reverse cycle heat-pump / air-conditioning to utilize the earth as both a heat source and a heat sink. we have focused on the opportunity to integrate heat exchanger pipework among the structural steel-reinforcement that is cast into basement walls and their underlying foundations. Such is a vertical planar foundation heat exchanger, referred to as diaphragm wall heat exchanger (DWHE).

Results of detailed simulations of a wide range of operating scenarios for DWHE systems have been presented in this paper, comparable with other DWHE designs described in the literature (Table 1). These results compared continuous full heat rejection/extraction into the foundation heat exchangers without any hybrid air-cooling capacity except for the heat transfer from diaphragm walls into basement exhaust ventilation systems.

Most of the tables of results were setup within guidelines whereby heat pump evaporator and chiller condenser water enter the heat exchangers between 1° and 37.8 °C, except Table 5 illustrates relaxation of the upper guideline – while retaining the rule to never operate within one degree of freezing. The upper guideline is the temperature of healthy human metabolism, which was devised because the diaphragm walls may adjoin underground parking areas suitable for pedestrian denizens.

Maximum tolerable basement wall temperatures impose an additional constraint not addressed by other studies. The present study assumed that these spaces are used for underground carparking and as a consequence of health and safety exhaust ventilation is employed with the result that evaporation of dampness resulted in entrained outdoor air temperature approaching wet-bulb. The forgoing could be described as a form of uncontrolled evaporative cooling that partially supplements the capacity of the earth as a heat sink.

Results are reported in the form of summary tables giving estimates of DWHE heat exchange potential for a prototypical office building in eight European cities, of which four are warm Mediterranean (Cfb), and four are cool Oceanic (Csa) – including continentally influenced examples (Cfb/BSk and Csb/Dfb). In the cooler locations, the foundation heat exchanger potential is limited by winter heat extraction, and so demand-side load reduction or supplemental heating are recommended where additional ground-source heat exchangers are not feasible.

In warm locations the foundation heat exchanger potential is limited by summer heat-rejection, and so supplemental cooling capacity may be needed. Additional cooling capacity could be provided via the demand-side such as by additional chillers or district cooling. Alternatively, additional heat rejection capacity could be added on the demand-side with hybrid control. The results presented show how the relationship between the DWHE system and the overall building

demand are related to system temperatures and overall system efficiencies. Conditions are identified in which system temperatures may become unacceptably high. These results demonstrate limits of potential performance in a prototypical system. We recommend that simulation studies are used in the detailed design stage of FHX projects to estimate likely performance and the best strategies for optimal operation.

This paper provides preliminary design guidelines for application of diaphragm wall heat exchangers in a range of European climates. For a prototypical office floorplan, we have found that two levels of basement diaphragm walls could enable geoexchange systems to serve one or more stories more than would have been accommodated with thermal piles alone.

Acknowledgments: This work was possible thanks to the research project H2020 GEOTeCH, funded by the European Union's Horizon 2020 research and innovation programme under grant agreement No 656889 (www.geotech-project.eu). Simon J Rees (SJR): Supervision, Project administration, Funding acquisition, and preliminary review. SJR lead Work Packages 3 and 5 of the GEOTeCH Project, and personally developed the diaphragm wall heat exchanger module for TRNSYS, compiling the Type5100 dynamic link libraries that access any given DTN file. SJR drafted the prototypical office building floor plan model in IES VE for generation of hourly heating and cooling loads.

Author Contributions: Eric L Peterson (ELP): Writing, literature review analysis, conceptualised the hydronic pipework and controls, parametric deckfiles for TRNSYS, postprocessing/visualization with Matlab, Design guidelines, Writing & Editing. ELP conceived of robust hydronics and controls to integrate ground-source heat exchangers with conventional building services if hourly load profiles and DTN files are provided. Ida Shafagh: DTN files production, writing and editing.

Nomenclature

bidecadal ΔT is the product of 20 years and the linear regression slope of fitting change of 20 successive annual average temperatures of foundation heat exchanger pipe wall.

$capacity_{concrete}$, the effective thermal capacity of concrete-reinforcement composite.

$capacity_{ground}$, the thermal capacity of ground outside diaphragm wall and below lowest basement.

Cfb, Köppen–Geiger Mediterranean climate

Cfb/BSk, Köppen–Geiger continentally influenced Mediterranean climate

Cover, the minimum horizontal thickness of concrete covering the outer diameter of FHX pipe.

C_p, the specific heat of heat transfer fluid. Water assumed as long as temperatures > 1 °C

Csa, Köppen–Geiger Oceanic climate

Csb/Dfb, Köppen–Geiger continentally influenced Oceanic climate

DEFAULT, the nominal case of FHX geometry whereby the serpentine pipework is cast within the entire diaphragm wall, 45% above and 55% below the lowest basement floor level.

$Depth_{basement}$, the vertical depth of lowest basement floor below outdoor ground surface.

$Depth_{wall}$, the vertical depth of concrete diaphragm wall foundation below outdoor ground surface.

DWHE, vertical diaphragm wall heat exchanger

f_{FHX}, the percentage ratio of activated number of FHX circuits divided by the number required to serve with nominal soil conductivity prevailing without need for hybrid air-coolers or cooling towers.

GEOTeCH, GEOthermal Technology for economic Cooling and Heating, European Union's Horizon 2020 research and innovation programme under grant agreement No 656889

HVAC, Heating, ventilation, and air-conditioning systems that maintain indoor climate of buildings.

$k_{concrete}$, the effective thermal conductivity of concrete-reinforcement composite.

k_{ground}, the thermal conductivity of ground outside diaphragm wall and below lowest basement.

n, the number of activated FHX circuits serving the building. These are 2.4 m_h wide in DEFAULT case.

m_v, Depth measured in units of meters parallel with vertical axis, positive downwards from the earth surface. Applies to depth of basement as well as the overall embedment depth of pipes (VL_{pipe}).

m_h, Horizontal measurement in units of meters of the diaphragm wall, typically building perimeter.

m_p, total serpentine meters length of embedded pipe circuit cast into any particular FHX module.

PipeSpacing, the horizontal centreline-to-centreline spacing (m_h) between vertical pipes of the FHX.

Q_{cap}, Rated capacity of reverse-cycle chiller/heat-pump, kW of heating or cooling load.

Q_{ssn}*, Design capacity of source-side network to accept the heat rejection of chiller or to cope with the heat extraction of the heat pump.

Q_{ssn}, Peak load imposed upon the source-side network if heatpump and chiller are simultaneously operating at full load with a blended confluence of flow from evaporator and condenser.

SPF_2, Seasonal performance factor including the source-side work of pumps and fans (if applicable).

$Thickness_{wall}$, the thickness of concrete enclosing the FHX pipework and structural reinforcement.

TRNSYS, University of Wisconsin's Transient System Simulation Tool – graphically based software environment used to simulate the transient behavior of renewable energy hydronics and HVAC.

UBO, a special case of FHX geometry whereby the serpentine pipework is cast under basement only.

unmet hours/yr is the 20-year average of the annual sum of hours for that stratified tank temperature outlets drops below 33°C on the supply to the building heating load or rises above 8°C on the supply to the building cooling load. Note 88 hours is equivalent to 1% of one year.

ΔT_{nom}, the magnitude of inlet-outlet fluid temperature difference through air-coolers.

ΔT_{FHX} is the design target for instantaneous temperature difference between the inlet and outlet of foundation heat exchanger pipework circuitry.

$Ø_{out}$, the outer diameter of FHX pipework cast within concrete diaphragm wall foundations.

$Ø_{in}$, the inside diameter of FHX pipework cast within concrete diaphragm wall foundations.

References

1. Shafagh, I., et al., *A Model of a Diaphragm Wall Ground Heat Exchanger.* Energies, 2020. **13**(2): p. 300.
2. Brandl, H., *Energy foundations and other thermo-active ground structures.* Geotechnique, 2006. **56**(2): p. 81-122.
3. Xia, C., et al., *Experimental study on geothermal heat exchangers buried in diaphragm walls.* Energy and buildings, 2012. **52**: p. 50-55.
4. Dong, S., et al., *Thermo-mechanical behavior of energy diaphragm wall: Physical and numerical modelling.* Applied Thermal Engineering, 2019. **146**: p. 243-251.
5. Sailer, E., et al., *Thermo-hydro-mechanical interactions in porous media: Implications on thermo-active retaining walls.* Computers and Geotechnics, 2021. **135**: p. 104121.
6. Sterpi, D., A. Coletto, and L. Mauri, *Investigation on the behaviour of a thermo-active diaphragm wall by thermo-mechanical analyses.* Geomechanics for Energy and the Environment, 2017. **9**: p. 1-20.
7. Zeng, S., Z. Yan, and J. Yang, *Review and forecast of ground heat exchangers development: A bibliometric analysis from 2001 to 2020.* Sustainable Energy Technologies and Assessments, 2021. **47**: p. 101547.
8. Esen, H., et al., *Energy and exergy analysis of a ground-coupled heat pump system with two horizontal ground heat exchangers.* Building and environment, 2007. **42**(10): p. 3606-3615.
9. Esen, H., M. Inalli, and M. Esen, *A techno-economic comparison of ground-coupled and air-coupled heat pump system for space cooling.* Building and environment, 2007. **42**(5): p. 1955-1965.
10. Rees, S.J., *An introduction to ground-source heat pump technology*, in *Advances in Ground-Source Heat Pump Systems*, S.J. Rees, Editor. 2016, Woodhead Publishing. p. 1-25.

11. Esen, H., et al., *Modeling a ground-coupled heat pump system by a support vector machine.* Renewable Energy, 2008. **33**(8): p. 1814-1823.
12. Di Donna, A., et al., *Energy performance of diaphragm walls used as heat exchangers.* Proceedings of the Institution of Civil Engineers-Geotechnical Engineering, 2017. **170**(3): p. 232-245.
13. Amis, T., *Energy piles and diaphragm walls.* Current and Future Research Into, 2010.
14. Sun, M., C. Xia, and G. Zhang, *Heat transfer model and design method for geothermal heat exchange tubes in diaphragm walls.* Energy and Buildings, 2013. **61**: p. 250-259.
15. Sterpi, D., G. Tomaselli, and A. Angelotti, *Energy performance of ground heat exchangers embedded in diaphragm walls: Field observations and optimization by numerical modelling.* Renewable Energy, 2020. **147**: p. 2748-2760.
16. Li, M., K. Zhu, and Z. Fang, *Analytical methods for thermal analysis of vertical ground heat exchangers*, in *Advances in Ground-Source Heat Pump Systems*, S.J. Rees, Editor. 2016, Woodhead Publishing. p. 157-183.
17. Yazuzturk, C. and J.D. Spitler, *A short time step response factor model for vertical ground loop heat exchangers.* Ashrae Transactions, 1999. **105**: p. 475.
18. Gao, J., et al., *Thermal performance and ground temperature of vertical pile-foundation heat exchangers: a case study.* Applied Thermal Engineering, 2008. **28**(17-18): p. 2295-2304.
19. En, C., *15450: Heating Systems in Buildings—Design of Heat Pump Heating Systems.* BSI Standards: Brussels, Belgium, 2007.
20. Sanner, B. *Standards and Guidelines for UTES/GSHP wells and boreholes*. in *14th International Conference on Energy Storage Adana*. 2018. Adana, TURKEY.
21. Bourne-Webb, P. *An overview of observed thermal and thermo-mechanical response of piled energy foundations*. in *European Geothermal Congress. Pisa, Italy*. 2013.
22. VDI, I., Verein Deutscher, *Thermische Nutzung des Untergrundes-Erdgekoppelte Warmepumpenalagen*, in *Part 2 Thermal use of the underground — Ground source heat pump systems*. 2001. p. 43.
23. Rees, S.J., *Horizontal and compact ground heat exchangers*, in *Advances in Ground-Source Heat Pump Systems*, S.J. Rees, Editor. 2016, Woodhead Publishing. p. 117-156.
24. Esen, H., M. Inalli, and M. Esen, *Technoeconomic appraisal of a ground source heat pump system for a heating season in eastern Turkey.* Energy Conversion and Management, 2006. **47**(9-10): p. 1281-1297.
25. Esen, H., M. Inalli, and M. Esen, *Numerical and experimental analysis of a horizontal ground-coupled heat pump system.* Building and environment, 2007. **42**(3): p. 1126-1134.
26. Esen, H., et al., *Performance prediction of a ground-coupled heat pump system using artificial neural networks.* Expert Systems with Applications, 2008. **35**(4): p. 1940-1948.
27. Esen, H., et al., *Modelling a ground-coupled heat pump system using adaptive neuro-fuzzy inference systems.* International Journal of Refrigeration, 2008. **31**(1): p. 65-74.
28. Esen, H., et al., *Artificial neural networks and adaptive neuro-fuzzy assessments for ground-coupled heat pump system.* Energy and Buildings, 2008. **40**(6): p. 1074-1083.
29. Esen, H., et al., *Forecasting of a ground-coupled heat pump performance using neural networks with statistical data weighting pre-processing.* International Journal of Thermal Sciences, 2008. **47**(4): p. 431-441.
30. Esen, H., et al., *Predicting performance of a ground-source heat pump system using fuzzy weighted pre-processing-based ANFIS.* Building and Environment, 2008. **43**(12): p. 2178-2187.
31. Esen, M. and T. Yuksel, *Experimental evaluation of using various renewable energy sources for heating a greenhouse.* Energy and Buildings, 2013. **65**: p. 340-351.
32. Esen, H., M. Esen, and O. Ozsolak, *Modelling and experimental performance analysis of solar-assisted ground source heat pump system.* Journal of Experimental & Theoretical Artificial Intelligence, 2017. **29**(1): p. 1-17.

33. Adam, D. and R. Markiewicz, *Energy from earth-coupled structures, foundations, tunnels and sewers.* Géotechnique, 2009. **59**(3): p. 229-236.
34. Cui, Y., J. Zhu, and F. Meng, *Techno-economic evaluation of multiple energy piles for a ground-coupled heat pump system.* Energy Conversion and Management, 2018. **178**: p. 200-216.
35. Di Donna, A., B. Marco, and A. Tony. *Energy Geostructures: Analysis from research and systems installed around the World*. in *42nd Annual Conference on Deep Foundations, New Orleans (USA)*. 2017.
36. Santamouris, M. and D. Kolokotsa, *Passive cooling dissipation techniques for buildings and other structures: The state of the art.* Energy and Buildings, 2013. **57**(Supplement C): p. 74-94.
37. Barla, M., A. Di Donna, and A. Perino, *Application of energy tunnels to an urban environment.* Geothermics, 2016. **61**: p. 104-113.
38. Barla, M., A. Di Donna, and A. Santi, *Energy and mechanical aspects on the thermal activation of diaphragm walls for heating and cooling.* Renewable Energy, 2018.
39. Bourne-Webb, P., T.B. Freitas, and R. da Costa Gonçalves, *Thermal and mechanical aspects of the response of embedded retaining walls used as shallow geothermal heat exchangers.* Energy and Buildings, 2016. **125**: p. 130-141.
40. GEOTeCH, G.T.f.E.C.a.H., *GEOTeCH - Barcelona Large Size pilot. Foundation Heat Exchanger (FHX)*. 2019: SOLINTEL M&P S. L., Edificio PAYMA, Avda. de la Industria 32, EP-2, 28108 Alcobendas – Madrid (SPAIN) & RINA Consulting – Dissemination, Via San Nazaro, 19. 16145 Genova (ITALY) https://www.youtube.com/watch?v=-2Iec6AY9C4.
41. Makasis, N. and G.A. Narsilio, *Energy diaphragm wall thermal design: The effects of pipe configuration and spacing.* Renewable Energy, 2020. **154**: p. 476-487.
42. Cui, W., S. Zhou, and X. Liu, *Optimization of design and operation parameters for hybrid ground-source heat pump assisted with cooling tower.* Energy and Buildings, 2015. **99**: p. 253-262.
43. Zhou, S., et al., *Design and operation of an improved ground source heat pump system assisted with cooling tower.* Procedia Engineering, 2017. **205**: p. 3214-3221.
44. Soga, K. and Y. Rui, *Energy geostructures*, in *Advances in Ground-Source Heat Pump Systems*, S.J. Rees, Editor. 2016, Woodhead Publishing. p. 185-221.
45. Kürten, S., D. Mottaghy, and M. Ziegler, *A new model for the description of the heat transfer for plane thermo-active geotechnical systems based on thermal resistances.* Acta Geotechnica, 2015. **10**(2): p. 219-229.
46. Zannin, J., et al., *Experimental analysis of a thermoactive underground railway station.* Geomechanics for Energy and the Environment, 2021: p. 100275.
47. Shafagh, I. and S.J. Rees. *A Foundation Wall Heat Exchanger Model and Validation Study*. in *IGSHPA, September 18-20, 2018*. 2018. Stockholm, Sweden.
48. Shafagh, I. and S.J. Rees. *Analytical Investigations into Thermal Resistance of Diaphragm Wall Heat Exchangers*. in *Proceedings of the European Geothermal Congress, EGC 2019*. 2019. EGEC Geothermal.
49. Di Donna, A., et al., *The role of ground conditions on the heat exchange potential of energy walls.* Geomechanics for Energy and the Environment, 2021. **25**: p. 100199.
50. Leeds, U.o., *Ground Heat Exchanger Technical and User Documentation*. 2018, GEOTeCH, Geothermal Technology for Economic Cooling and Heating
51. American Society of Heating, R. and A.-C. Engineers, *International Weather for Energy Calculations (IWEC Weather Files) User's Manual*. 2001, ASHRAE Atlanta, GA.
52. Klein, S., et al., *Mathematical Reference*, in *TRNSYS 17: A Transient System Simulation Program. Solar Energy Laboratory*. 2014, University of Wisconsin, : Madison, USA.
53. Claesson, J. *Dynamic thermal networks: a methodology to account for time-dependent heat conduction*. 2003.

54. Claesson, J. and S. Javed, *A load-aggregation method to calculate extraction temperatures of borehole heat exchangers.* ASHRAE Transactions, 2012. **118**(1): p. 530-539.
55. Beier, R.A. and J.D. Spitler, *Weighted average of inlet and outlet temperatures in borehole heat exchangers.* Applied energy, 2016. **174**: p. 118-129.
56. UNIVLEEDS, *Appendix 6: DTN Weighting Factor Calculation Tool. Ground Heat Exchanger Technical and User Documentation* in *GEOthermal Technology for economic Cooling and Heating (GEOTeCH)*. 2017, University of Leeds.
57. Mitchell, M.S. and J.D. Spitler, *Characterization, Testing and Optimization of Load Aggregation Methods for Ground Heat Exchanger Response-Factor Models.* Science and Technology for the Built Environment, 2019: p. 1-21.
58. Perez Gonzalez, J.A., *Understanding numerically generated g-functions: A study case for a 6x6 borehole field*. 2013.
59. Eskilson, P., *Thermal analysis of heat extraction boreholes.* 1987.
60. Dusseault, B., P. Pasquier, and D. Marcotte, *A block matrix formulation for efficient g-function construction.* Renewable Energy, 2018. **121**: p. 249-260.
61. Fan, D., S. Rees, and J. Spitler, *A dynamic thermal network approach to the modelling of foundation heat exchangers.* Journal of Building Performance Simulation, 2013. **6**(2): p. 81-97.
62. UNIVLEEDS, *Appendix 5: Numerical Step-response Calculation Tool. Ground Heat Exchanger Technical and User Documentation* in *GEOthermal Technology for economic Cooling and Heating (GEOTeCH)*. 2017, University of Leeds.
63. Arteconi, A., N.J. Hewitt, and F. Polonara, *Domestic demand-side management (DSM): Role of heat pumps and thermal energy storage (TES) systems.* Applied thermal engineering, 2013. **51**(1-2): p. 155-165.
64. DIN16893, D.I.f.N., *DIN 16893 Crosslinked polyethylene (PE-X) pipes - Dimensions; Text in German and English*, in *This standard has been prepared by Technical Committee Außendurchmesser und Betriebsüberdrücke of the Normenausschuss Kunststoffe (Plastics Standards Committee)*. 2019.
65. UNIVLEEDS, *Appendix 3: Screen wall parametric mesh generation tool. Ground Heat Exchanger Technical and User Documentation*, in *GEOthermal Technology for economic Cooling and Heating (GEOTeCH)*. 2017, University of Leeds.

List of Figure Legends

Figure 1.

Four-pipe heatpump/chiller with demand-side buffer tanks and hybrid source-side heat exchangers. The air-cooled mode is not considered in the current paper. Serpentine diaphragm wall heat exchanger sections are repeated in parallel with common entering and leaving headers. Graphic courtesy Simon Rees, Professor of Building Energy Systems, University of Leeds.

Figure 2.

Definition of the three boundary surfaces and corresponding time-varying heat fluxes in a Dynamic Thermal Network (DTN) representation of a diaphragm wall ground heat exchanger. Reproduced from Shafagh and Rees' [1] – Creative Commons (CC BY 4.0).

Figure 3.

Geoexchange system, with building demand-side on the left of heat-pump and chiller, and source-side confluence of water circuits through the heat pump evaporator and chiller condenser. Reject streams of heat-pump and chiller may run alternatively or blended simultaneously at "mixSSN". Source-side allows hybrid control with air-source DryCooler - not considered at present.

Figure 4.

Diaphragm wall heat exchanger with pipes fitted below the basement level [65].

Figure 5.

Pipe depth from the ground surface (DEFAULT) diaphragm wall heat exchanger [65].

Figure 6:

Prototypical office building. Two levels of underground carpark (brown) diaphragm wall foundation heat exchangers (FHX) are assumed. Above ground level (green) denotes replicated office floors which might be served by reverse-cycle ground-source heat pumps served by the limited FHX availability. Higher levels (blue) denote additional office levels which would require hybrid air-coolers to supplement FHXs, district cooling, or rooftop air-cooled chillers.

Figure 7.

Part-load histograms from Mediterranean sites (upper pane) and Oceanic sites (lower pane) for the same prototypical office building floorplan. The range of heat-pump/chiller capacity was divided into 30 bins plotted across the horizontal axis. Frequency of hourly part-load occurrences is plotted in the vertical axis, where blue denotes cooling and orange denotes heating. The insets have vertical scale zoomed to 100 hours per annum, to resolve high loading. Boxes span between minimum and maximum, circles contain median, and crosses mark average of 3 values.

Figure 8.

Barcelona example annual average simulation results with continuous heat injection and/or heat extraction through FHX circuits. Nominal soil conductivity (1.6 W/m·K). These plots present simulated annual energy metering without any air-cooling, entirely geo-exchange operation for 20 years.